



OPEN ACCESS

EDITED BY

Rongrui Wei,
Jiangxi University of Traditional Chinese
Medicine, China

REVIEWED BY

Feng Zhang,
Nanjing University of Chinese Medicine, China
Mengnan Liu,
Southwest Medical University, China

*CORRESPONDENCE

Jinhao Zeng,
✉ zengjinhao@cdutcm.edu.cn
Yu Chen,
✉ 735405661@qq.com
Xiao Ma,
✉ tobymaxiao@cdutcm.edu.cn

[†]These authors have contributed equally to this work and share first authorship

RECEIVED 10 October 2023

ACCEPTED 08 January 2024

PUBLISHED 29 January 2024

CITATION

Feng W, Kao T-c, Jiang J, Zeng X, Chen S, Zeng J, Chen Y and Ma X (2024), The dynamic equilibrium between the protective and toxic effects of matrine in the development of liver injury: a systematic review and meta-analysis. *Front. Pharmacol.* 15:1315584. doi: 10.3389/fphar.2024.1315584

COPYRIGHT

© 2024 Feng, Kao, Jiang, Zeng, Chen, Zeng, Chen and Ma. This is an open-access article distributed under the terms of the [Creative Commons Attribution License \(CC BY\)](https://creativecommons.org/licenses/by/4.0/). The use, distribution or reproduction in other forums is permitted, provided the original author(s) and the copyright owner(s) are credited and that the original publication in this journal is cited, in accordance with accepted academic practice. No use, distribution or reproduction is permitted which does not comply with these terms.

The dynamic equilibrium between the protective and toxic effects of matrine in the development of liver injury: a systematic review and meta-analysis

Weiyei Feng^{1,2,3†}, Te-chan Kao^{1,2,3†}, Jiajie Jiang^{1,2,3†}, Xinyu Zeng^{2,4}, Shuang Chen^{2,4}, Jinhao Zeng^{1,3,5*}, Yu Chen^{1,3,5*} and Xiao Ma^{2,4*}

¹TCM Regulating Metabolic Diseases Key Laboratory of Sichuan Province, Hospital of Chengdu University of Traditional Chinese Medicine, Chengdu, China, ²State Key Laboratory of Southwestern Chinese Medicine Resources, Chengdu University of Traditional Chinese Medicine, Chengdu, China, ³School of Clinical Medicine, Chengdu University of Traditional Chinese Medicine, Chengdu, China, ⁴School of Pharmacy, Chengdu University of Traditional Chinese Medicine, Chengdu, China, ⁵Hospital of Chengdu University of Traditional Chinese Medicine, Chengdu, China

Background: Matrine, an alkaloid derived from the dried roots of *Sophora flavescens* Aiton, has been utilized for the treatment of liver diseases, but its potential hepatotoxicity raises concerns. However, the precise condition and mechanism of action of matrine on the liver remain inconclusive. Therefore, the objective of this systematic review and meta-analysis is to comprehensively evaluate both the hepatoprotective and hepatotoxic effects of matrine and provide therapeutic guidance based on the findings.

Methods: The meta-analysis systematically searched relevant preclinical literature up to May 2023 from eight databases, including PubMed, Web of Science, Cochrane Library, Embase, China National Knowledge Infrastructure, WanFang Med Online, China Science and Technology Journal Database, and China Biomedical Literature Service System. The CAMARADES system assessed the quality and bias of the evidence. Statistical analysis was conducted using STATA, which included the use of 3D maps and radar charts to display the effects of matrine dosage and frequency on hepatoprotection and hepatotoxicity.

Results: After a thorough screening, 24 studies involving 657 rodents were selected for inclusion. The results demonstrate that matrine has bidirectional effects on ALT and AST levels, and it also regulates SOD, MDA, serum TG, serum TC, IL-6, TNF- α , and CAT levels. Based on our comprehensive three-dimensional analysis, the optimal bidirectional effective dosage of matrine ranges from 10 to 69.1 mg/kg. However, at a dose of 20–30 mg/kg/d for 0.02–0.86 weeks, it demonstrated high liver protection and low toxicity. The molecular docking analysis revealed the interaction between MT and SERCA as well as SREBP-SCAP complexes. Matrine could alter Ca²⁺ homeostasis in liver injury via multiple pathways, including the SREBP1c/SCAP, Notch/RBP-J/HES1, I κ K/NF- κ B, and Cul3/Rbx1/Keap1/Nrf2.

Conclusion: Matrine has bidirectional effects on the liver at doses ranging from 10 to 69.1 mg/kg by influencing Ca²⁺ homeostasis in the cytoplasm, endoplasmic reticulum, Golgi apparatus, and mitochondria.

Systematic review registration: <https://inplasy.com/>, identifier INPLASY202340114

KEYWORDS

matrine, hepatotoxicity, hepatoprotection, liver injury, meta-analysis

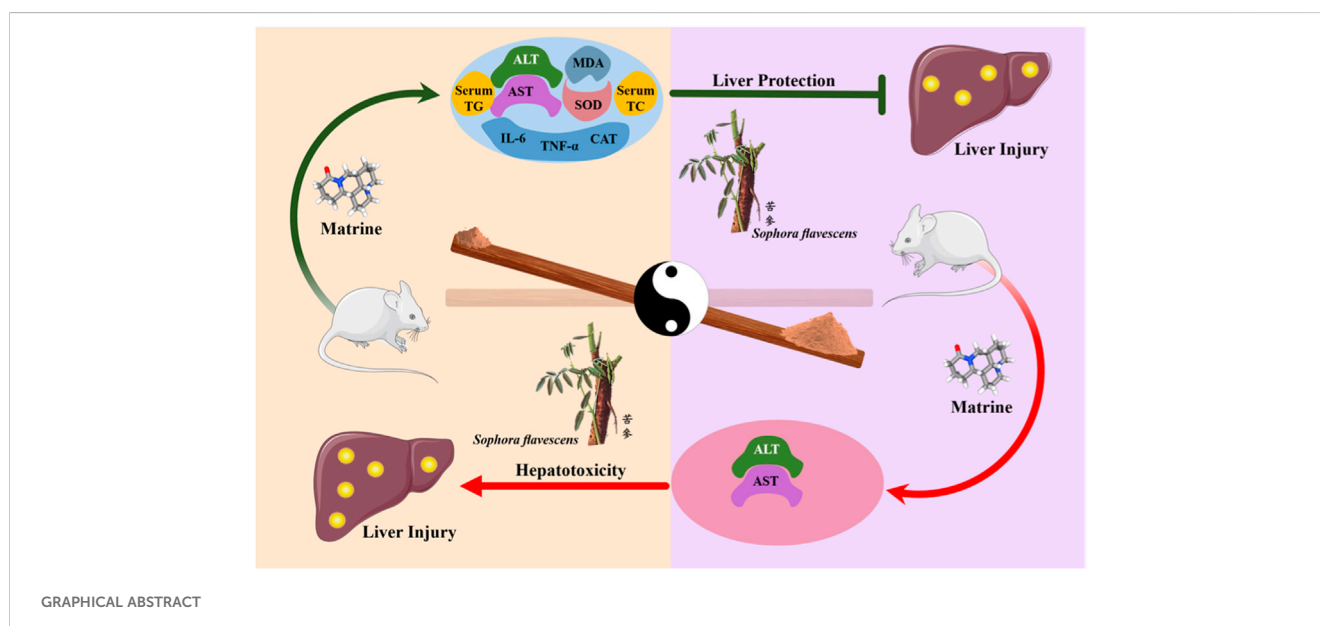
1 Introduction

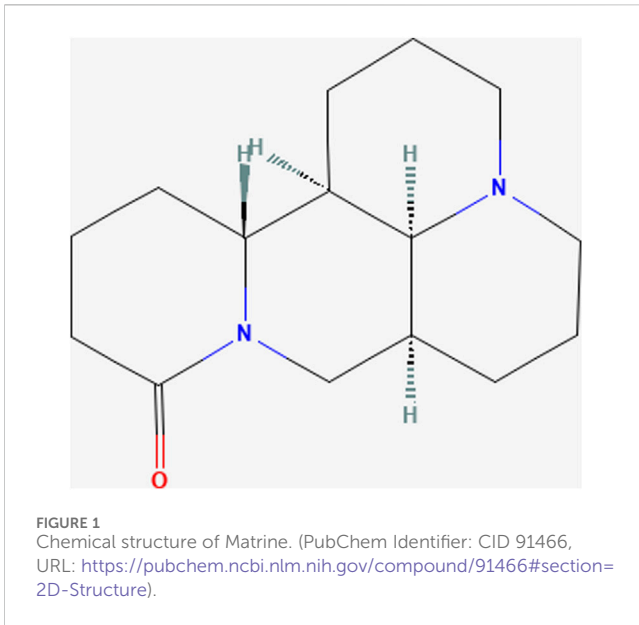
Liver injury (LI) is a prevalent liver disease and a significant global health concern due to its high mortality rates. The European Association for the Study of the Liver (EASL) has reported that liver disease ranks 11th as the leading cause of death worldwide, accounting for 4% of all deaths. In 2023, Devarbhavi et al. estimated over two million fatalities annually due to liver disease (Devarbhavi et al., 2023). As a preliminary stage of liver disease, LI can be caused by various factors such as alcohol, infection, immunity, and drug-induced toxicity (Younossi et al., 2023). The severity of LI can range from mild inflammation to more severe conditions like liver cirrhosis, liver failure and even death. Symptoms of LI consist of abnormalities in liver function test abnormalities, fever, nausea, vomiting, jaundice, and right epigastric pain (Knight, 2005). Hepatocellular damage, fibrosis, and inflammatory infiltration are key pathological features of LI. Anti-viral drugs, liver protective agents, and immunosuppressive drugs are the mainstream drugs used to treat LI. While corticosteroids, pioglitazone, cholestyramine, and other medications are commonly prescribed to treat different types of LI (Devarbhavi et al., 2023), their hepatotoxicity can lead to drug-induced liver injury (DILI) in clinical settings. Therefore, exploring more effective and safer alternatives for LI is necessary.

The dried roots of *Sophora flavescens* Aiton (well-documented in The Plant List www.theplantlist.org), a Traditional Chinese Medicine (TCM) herb, commonly known as KuShen, was initially discovered for its therapeutic properties in the ancient text *Shen Nong Ben Cao Jing*. For thousands of years, the dried roots of *S. flavescens* Aiton has been widely used to treat various digestive disorders, such as dysentery, bloody stools, jaundice, and especially liver diseases (Chinese Pharmacopoeia Commission,

2020). Kushen Decoction and Longdan Kushen Decoction are the representative TCM prescriptions that incorporate the dried roots of *S. flavescens* Aiton for treating liver disease. Contemporary pharmacological studies have revealed that extracts of the dried roots of *S. flavescens* Aiton have hepatoprotective effects due to their anti-inflammatory and antiviral properties (He et al., 2015).

Matrine ((1R,2R,9S,17S)-7,13-diazatetracyclo [7.7.1.02,7.013,17] heptadecan-6-one; $C_{15}H_{24}N_2O$; MW = 248.36) is an alkaloid extracted from the dried roots of *S. flavescens* Aiton and can be dissolved in various solvents such as water, ethanol, benzene, etc. (Sun et al., 2022). As an active ingredient of the dried roots of *S. flavescens* Aiton, the total content of matrine and oxymatrine should not be less than 1.2% according to the Pharmacopoeia of the People's Republic of China (Chinese Pharmacopoeia Commission, 2020). Numerous studies have shown that MT has anti-inflammatory, anti-viral, anti-tumor, and immune-suppressive abilities (Zhou et al., 2014; Wang et al., 2018; Peng et al., 2020; Chu et al., 2021; Jing et al., 2021). MT has been reported to regulate liver protective function, hepatic regeneration, and alleviate LI through several signaling pathways, such as TGF- β /Smad, NF- κ B, Wnt/ β -catenin, Notch/Jagged1/recombination signal binding protein for immunoglobulin kappa J (RBP-J κ , RBP-J)/hairly and enhancer of split-1 (HES1) (Yu H. B. et al., 2011; Yu et al., 2014; Yang et al., 2016; Yin et al., 2018). Due to its extensive pharmacological effects, MT is often used as an injection in clinical practice for hepatitis B, tumors, and immune diseases (Liu and Zhang, 2021). In the clinical pharmacokinetic study of MT, serum MT concentrations ranged from 1 to 6 μ g/mL after a large-dose intravenous infusion (6 mg/kg) (Zhang et al., 2009). In rats, the maximum blood concentration of MT was found to reach $2,412 \pm 362$ ng/mL and 94.6 ± 38.6 ng/mL after intravenous or oral





administration of MT at a dose of 2 mg/kg (Yang et al., 2010). However, in recent years, several studies have demonstrated that MT can lead to DILI, reproductive toxicity, and neurotoxicity (Wang et al., 2017). MT has been demonstrated to induce hepatotoxicity through inhibiting the Nrf2 pathway and stimulating the reactive oxygen species (ROS)-mediated mitochondrial apoptosis pathway (You et al., 2019). Nevertheless, the mechanisms of MT in liver protection and hepatotoxicity are continually being improved and elucidated (Figure 1).

Calcium ion (Ca^{2+}), a multifunctional intracellular messenger, affects cellular metabolism, energy generation, and intracellular homeostasis under physiological conditions. Extracellular stress stimulation on the cell membrane could enhance Ca^{2+} influx, and increased cytoplasmic Ca^{2+} would be transported into the Endoplasmic reticulum (ER) lumen and stored via cross specific Ca^{2+} ion channels, such as sarcoendoplasmic reticulum calcium transport ATPase (SERCA) (Periasamy and Kalyanasundaram, 2007; Chemaly et al., 2018). Loss of Ca^{2+} homeostasis and irregular Ca^{2+} channels on the cell membrane, ER, and mitochondria might cause ER stress and modify the mitochondrial membrane potential, raising total ROS in hepatocytes (Kaufman and Malhotra, 2014; Zeeshan et al., 2016). Based on the current literature, distinct MT concentration gradients can influence diverse SERCA responses on the ER, regulate mitochondrial activity, and balance intracellular Ca^{2+} levels to alleviate or promote hepatocyte stress (Gao et al., 2019).

Previous studies have demonstrated that MT exhibits both hepatoprotective effects and the potential to cause liver damage, yet the underlying mechanisms remain unclear. Therefore, the objective of this study is to conduct a systematic review and meta-analysis to investigate the impact of MT on LI and elucidate the dynamic processes through which MT leads to liver protection and hepatotoxicity. Additionally, this study aims to explore the role of Ca^{2+} in these processes, offering innovative insights into the mechanisms involved.

2 Methods

2.1 Registration of the meta-analysis

The meta-analysis followed the PRISMA 2020 guidelines and has been submitted to the International Platform of Registered Systematic Review and Meta-analysis Protocols (INPLASY) database (<https://inplasy.com/>). The registration number for this submission is INPLASY202340114.

2.2 Data sources and search strategy

The retrieved databases included four English databases and four Chinese databases according to the five articles (Ju et al., 2018; Xiong et al., 2019; Liu et al., 2021; Luo et al., 2021; Zheng et al., 2021). The four English databases were: PubMed, Web of science, Cochrane library, Embase. And the four Chinese databases: China National Knowledge Infrastructure, WanFang Med Online, China Science and Technology Journal Database, and China Biomedical Literature Service System. The literature search in this study encompassed all pertinent literature up until May 2023.

The search terms were “Matrine,” “liver injury,” “hepatoprotection,” and “hepatotoxicity”. (Figure 2 and Supplementary Table S1).

2.3 Included criteria and excluded criteria

Considering the difference between hepatotoxicity and hepatoprotection of MT, this article has formulated appropriate included and excluded criteria to address these dual effects.

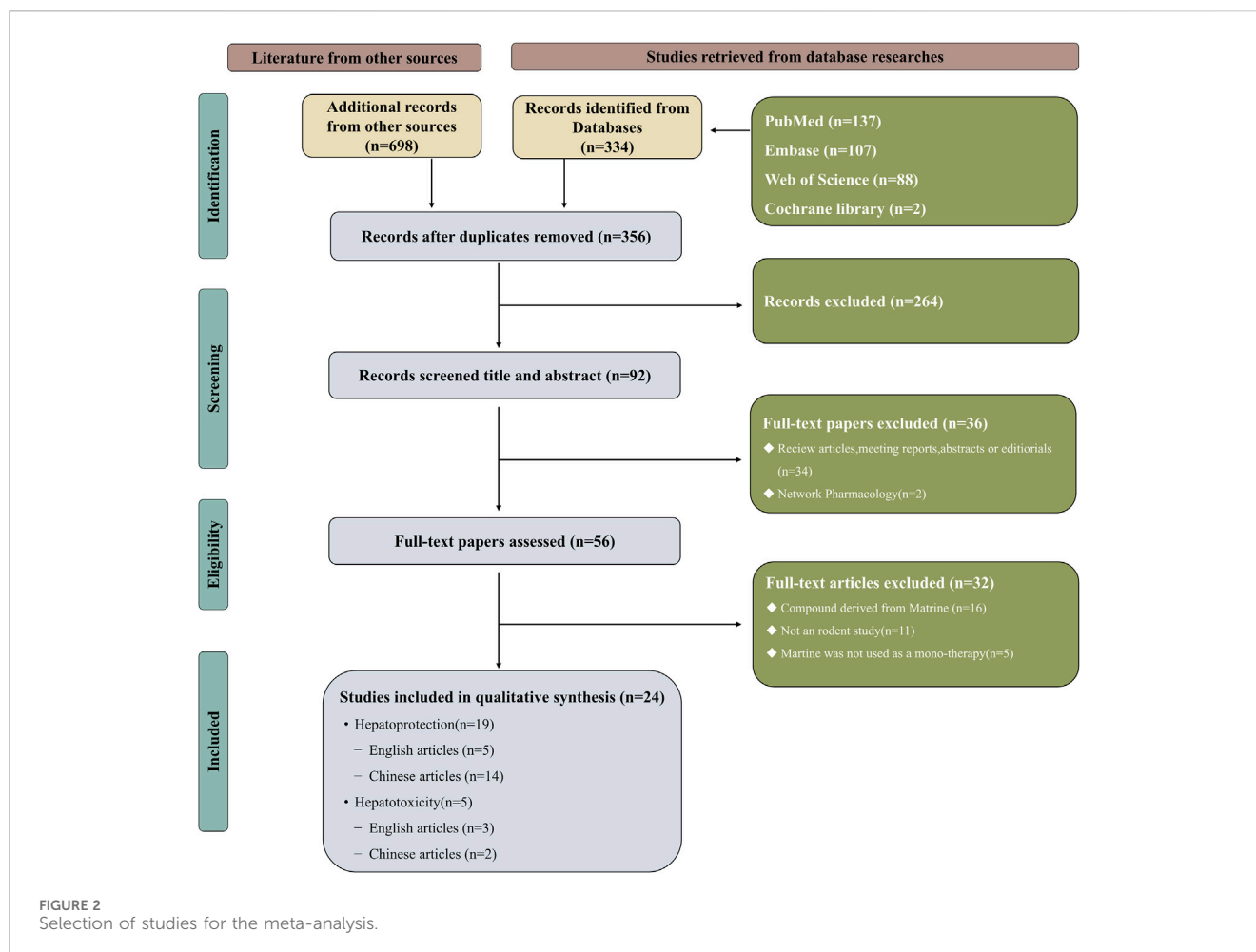
2.3.1 Included criteria

Research of hepatoprotection needs to meet the following requirements: 1) Subjects: the study involved rats or mice as the population. 2) Control(C) group and intervention(I) group: each study included at least 1 LI group as the C group and 1 MT group as the I group. 3) The I groups were comprised of LI models and received MT monotherapy exclusively. The C groups consisted of LI models that either received no treatment or received non-functional intervention. 4) The indicators of the studies should encompass AST, ALT, MDA, SOD, serum TG, serum TC, IL-6, CAT, and TNF- α , either in their entirety or partially. 5) The quality evaluation results were above 5 points.

Research of hepatotoxicity needs to meet the following requirements: 1) Subjects: the study involved rats or mice as the population. 2) C group and I group: each study included at least 1 LI group as the C group and 1 MT group as the I group. 3) The I groups were comprised of normal animals and received MT monotherapy exclusively. The C groups consisted of normal animals that either received no treatment or received non-functional intervention. 4) The indicators of the studies should encompass AST and ALT, either in their entirety or partially. 5) The quality evaluation results were above 5 points.

2.3.2 Excluded criteria

Excluded criteria for the research of hepatoprotection: 1) LI rats or mice were not selected as animal subjects for hepatoprotection



studies. 2) The experiments did not form controls. 3) The I group did not receive MT monotherapy. The C group used functional drugs (including Western medicines, TCMs and integrative medicines) as interventions, and could not provide specific outcome indices. 4) The common indicators of LI were not included in the study. 5) Quality evaluation results below 5 points.

Excluded criteria for the research of hepatotoxicity: 1) Normal rats or mice were not selected as subjects for hepatotoxicity studies. 2) The experiments did not form controls. 3) The I group did not receive MT monotherapy. The C group used functional drugs (including Western medicines, TCMs and integrative medicines) as interventions, and could not provide specific outcome indices. 4) The common indicators of LI were not included in the study. 5) Quality evaluation results below 5 points.

2.4 Data extraction

Two researchers extracted the following data from the included articles: 1) The first author's name and publication year; 2) Basic animal characteristics: including the number, species (mice or rats), strain, sex, and weight; 3) Modeling details: including the method of modeling and criteria for successful modeling; 4) Specific

intervention methods: including the drug used, dosage, and frequency of administration; 5) Outcome measures. (Table 1).

Regarding the preset indicators, we recorded only the highest dose group in the gradient dosages. For the experiments that observed data from multiple time points, only the last were recorded. We collected the experimental data by Universal Desktop Ruler and calculated the mean and standard deviation (SD) of the continuous variables. Results of the measurements were displayed in graphics rather than digital text.

2.5 Risk of bias and quality of evidence

The CAMARADES (Collaborative Approach to Meta-Analysis and Review of Animal Data from Experimental Studies) 10-point scoring scale, an internationally recognized criteria published in 2004, is utilized to assess and calculate a methodological quality score (Macleod et al., 2004). Two researchers made an independently assessment of the methodological quality of the surveys. The quality measures were changed in accordance with the study's specificity. When there was a disagreement in the evaluation, the correspondence author came to an agreement or used arbitration. The specific methods were also provided in Figure 3.

TABLE 1 The key characteristics of all 24 Studies.

Author(s)/Year	Species	Gender (M/F)	Weight of the animal	Sample size (n)MT/Model	Drug dosage	Treatment courses	Main outcome indicators
Song2009	Kunming mice	NM	18–22 g	12/12	MT: MT,62.5 mg/kg	10 days	ALT, AST
					Mod: No drugs		
Liang2015	ICR mice	Female and male	18–22 g	10/10	MT: MT,40 mg/kg	60 days	ALT, AST
					Mod: Equal volume water		
Gu2019	C57BL/6 mice	Male	18–20 g	11/10	MT: MT,69.1 mg/kg	90days	ALT, AST
					Mod: Distilled water (constant volume)		
Liu2020	BALB/c mice	Male	17.7–18.1 g	10/10	MT: MT,100 mg/kg	1 week	ALT, AST
					Mod: Normal saline		
Rao2022	ICR mice	Male	18–22 g	10/10	MT: MT,60 mg/kg	2 weeks	ALT, AST
					Mod: Normal saline		
Li2005	NIH mice	Male	18–22 g	10/10	MT: Con A,20 mg/kg + MT,25 mg/kg	3 days	ALT, TNF- α
					Mod: Con A,20 mg/kg		
Liu2008	Sprague Dawley rats	Male	210–230 g	92/92	MT: HIRI + MT,60 mg/kg	1 day	ALT, AST, IL-6, TNF- α
					Mod: HIRI		
Zhou2009	NIH mice	Male	18–22 g	13/11	MT: Con A,20 mg/kg + MT,25 mg/kg	5 days	ALT, AST
					Mod: Con A,20 mg/kg		
Yang2013	Sprague Dawley rats	Male	180–220 g	24/24	MT: 2-AAF, 15 mg/kg + MT,20 mg/kg	3 weeks	ALT
					Mod: 2-AAF, 15 mg/kg		
Shi2013	C57BL/6 mice	Female	NM	8/8	MT: CCl ₄ ,0.6 mL/kg + MT,30 mg/kg	6 weeks	ALT
					Mod: CCl ₄ ,0.6 mL/kg		
Zhang2013	Wistar rats	Male	180–200 g	6/6	MT: High-fructose diet + MT,160 mg/kg	4 weeks	ALT, AST, Serum TG, TNF- α , CAT, MDA, SOD
					Mod: High-fructose diet		
Gao2013	Sprague Dawley rats	Female and male	100–140 g	12/12	MT: Chinese liquor,43% vol + MT, 50 mg/kg	30 days	ALT, AST, Serum TG, Serum TC, CAT, MDA, SOD
					Mod: Chinese liquor,43% vol		
Tang2013	Wistar rats	Female and male	113–118 g	10/10	MT: High fatty diet + MT,36 mg/kg	30 days	Serum TG, Serum TC
					Mod: High fatty diet		
Wu2014	Kunming mice	Male	18–22 g	10/10	MT: ethanol,5 g/kg + MT,80 mg/kg	6 days	ALT, AST, MDA, SOD
					Mod: ethanol,5 g/kg		
Zhu2015	Sprague Dawley rats	Male	200–250 g	15/15	MT: HIRI + MT,30 mg/kg	4 h	ALT, AST, TNF- α
					Mod: HIRI		
Zhao2015	Wistar rats	Male	180–220 g	12/12	MT: CCl ₄ ,1 mL/kg + MT,10 mg/kg	1 week	ALT, AST, TNF- α
					Mod: CCl ₄ ,1 mL/kg		

(Continued on following page)

TABLE 1 (Continued) The key characteristics of all 24 Studies.

Author(s)/Year	Species	Gender (M/F)	Weight of the animal	Sample size (n)MT/Model	Drug dosage	Treatment courses	Main outcome indicators
Li2016	Sprague Dawley rats	Female and male	100–140 g	12/12	MT: Chinese liquor,43% vol + MT, 100 mg/kg	30 days	ALT, AST, Serum TG, Serum TC, CAT, MDA, SOD
					Mod: Chinese liquor,43% vol		
Guo2017	Sprague Dawley rats	Male	180–220 g	8/8	MT: CCl ₄ ,3 mL/kg + MT,72.8 mg/kg	3 weeks	ALT, AST
					Mod: CCl ₄ ,3 mL/kg		
Gao2018	C57BL/6 mice	Male	NM	10/10	MT: High-fat diet + MT,10 mg/kg	7 weeks	ALT, AST, Serum TG, Serum TC, TNF- α
					Mod: High-fat diet		
Bai2018	Sprague Dawley rats	Male	200–250 g	10/10	MT: HIRI + MT,50 mg/kg	4 h	ALT, AST, TNF- α
					Mod: HIRI		
Khan2019	BALB/c mice	Male	24–35 g	5/5	MT: CCL ₄ ,1 mL/kg + MT,50 mg/kg	1 day	ALT, AST, MDA
					Mod: CCL ₄ ,1 mL/kg		
Yuan2020	Sprague Dawley rats	Male	200–250 g	6/6	MT: HIRI + MT,40 mg/kg	1 week	ALT, AST, MDA, SOD
					Mod: HIRI		
Chang2021	C57BL/6 mice	Male	18–22 g	8/8	MT: acetaminophen,400 mg/kg + MT,2.8 mg/kg	1 week	ALT, AST, TNF- α , MDA, SOD
					Mod: acetaminophen, 400 mg/kg		
Du2021	Kunming mice	Male	18–22 g	6/6	MT: ethanol,5.4 g/kg + MT,2.8 mg/kg	2 weeks	ALT, AST, CAT, MDA, SOD
					Mod: ethanol,5.4 g/kg		

Abbreviations: Green area: in the matter of hepatotoxicity of MT (n = 5); Yellow area: in the matter of hepatoprotection of MT (n = 19) NM, not mentioned; ICR, Institute of Cancer Research; MT, matrine; **Mod**, model; 2-AAF, N-2-acetylaminofluorene; **HIRI**, hepatic ischemia-reperfusion injury (clip-closed portal vein and hepatic artery followed by reperfusion); **ALT**, alanine aminotransferase; **AST**, aspartate aminotransferase; **IL-6**, interleukin-6; **TNF- α** , tumor necrosis factor alpha; Serum TG, serum triglyceride; **Serum TC**, serum cholesterol; **CAT**, catalase; **SOD**, superoxide dismutase; **MDA**, malondialdehyde.

2.6 The dose-time-effect relationship and mechanism analysis of MT

To visualize the dose-time-effect relationship for hepatoprotection and hepatotoxicity of MT, this study unified the time units of all experiments into weeks (W), as well as constructed 3D maps and radar charts. In addition, the regulatory mechanism of MT role in the literature is summarized.

deemed to exhibit significant heterogeneity when I^2 exceeded 50%. Investigators conducted subgroup analyses for animal species (rat, mouse), dose administered (low (L) \leq 25 mg/kg, 25<medium (M) \leq 50 mg/kg, high (H) $>$ 50 mg/kg), and time of administration ($<$ 4w, \geq 4w) in order to identify the source of heterogeneity. To establish whether the findings were trustworthy enough to draw inferences, sensitivity analysis was done.

2.7 Quantitative synthesis and statistical analyses

Statistical analysis of indicators in this study was conducted using STATA 16.0 software. When the results are statistically significant, the p -value should be less than 0.05 ($p < 0.05$). Results were quantified using the standardized mean differences (SMD) and accompanying 95% confidence intervals (95% CI). The I-squared (I^2) test was used to assess the degree of heterogeneity and consistency between research (random-effects model [$I^2 > 50\%$] or fixed-effects model [$I^2 \leq 50\%$]). Results were

2.8 Molecular docking

The compounds and ligands were obtained from the PubChem database (<https://pubchem.ncbi.nlm.nih.gov>) and RCSB Protein Data Bank database (<https://www.rcsb.org/structure>). Molecular docking was performed using AutoDockTools 1.5.6 and AutoDock Vina 4.2. Here is a brief summary of the docking process.

1) The structure of MT was downloaded from the PubChem database. It was then converted into a 3D structure using ChemDraw software to minimize the structural energy. The 3D structure was calculated using AutoDockTools 1.5.6 software and

Category	First author	Publication year	A	B	C	D	E	F	G	H	I	J	Total
hepatotoxicity (n=5)	Bing Song	2009	√	√	√	√			√	√		√	7
	Pei Liang	2015	√	√	√	√			√	√		√	7
	Yingmin Gu	2019	√	√	√	√		√	√	√	√	√	9
	Jie Liu	2020	√		√	√			√	√	√	√	7
	Siwei Rao	2021	√	√	√	√			√	√	√	√	8
Hepatoprotection (n=19)	Changqing Li	2005	√		√	√			√	√		√	6
	Hao Liu	2008	√		√	√			√	√		√	6
	Minchao Zhou	2009	√	√	√	√			√	√		√	7
	Zhiyun Yang	2013	√	√	√	√			√	√	√	√	8
	Bin Tang	2013	√	√	√	√			√	√	√	√	8
	Duo Shi	2013	√	√	√	√		√	√	√	√	√	9
	Hefang Zhang	2013	√	√	√	√		√	√	√	√	√	9
	Yan Gao	2013	√	√	√	√			√	√	√	√	8
	Yang Wu	2014	√	√	√	√			√	√	√	√	8
	Jun Zhu	2015	√	√	√	√		√	√	√	√	√	9
	Yan Zhao	2015	√		√	√			√	√	√	√	7
	Xiaohua Li	2016	√	√	√	√			√	√	√	√	8
	Shun Guo	2017	√	√	√	√			√	√	√	√	8
	Xiaobo Gao	2018	√	√	√	√			√	√	√	√	8
	Ning Bai	2018	√	√	√	√		√	√	√	√	√	9
	Adnan Khan	2019	√	√	√	√		√	√	√	√	√	9
	Fang Yuan	2020	√	√	√	√			√	√		√	7
	Lele Chang	2021	√	√	√	√			√	√	√	√	8
	Mengfan Du	2021	√	√	√	√			√	√	√	√	8

A: peer reviewed publication; B: control of temperature; C: random allocation to treatment or control; D:construct suitable animal models according to the purpose of the study; E: blinded assessment of outcome; F: use of anesthetic without significant intrinsic neuroprotective activity; G: animal model (rats or mice); H: sample size calculation; I: compliance with animal welfare policies; and J: statement of potential conflict of interests.

FIGURE 3 Risk of bias and quality assessment scores in each study.

saved as a pdbqt file. 2) The ligands were obtained from the RCSB protein bank. They were imported into PyMOL, dehydrated, hydrogenated, and prepared for ligand separation. The docking grid box was constructed in AutoDockTools 1.5.6 at the active site for each target protein and saved in pdbqt format. 3) AutoDock Vina 1.1.2 was used for molecular docking of the potential targets and active compounds, as well as to evaluate free binding energies. 4) PyMOL 2.6 and Discovery Studio 2019 were utilized for visualizing and analyzing interactions.

3 Results

3.1 Comprehensive literature review and selection

By using keywords, 1,032 articles in all could be found (334 articles from the four English databases and 698 articles from the four Chinese databases). After eliminating 676 duplicate articles, the researchers further examined the rest 356 articles. Depending upon the inclusion and exclusion criteria, the researchers excluded 264 articles after reviewing the titles and abstracts. And 34 articles on MT reviews, conference reports, abstracts or editorials and web pharmacology were subsequently eliminated from consideration. The remaining 32 articles were excluded after reviewing the full text. This meta-analysis eventually comprised 24 publications, 16 of which were in Chinese (Li et al., 2005; Liu et al., 2008; Song et al., 2009; Zhou et al., 2009; Gao et al., 2013; Tang et al., 2013; Wu et al., 2014; Liang et al., 2015; Zhao, 2015; Zhu et al., 2015; Li et al., 2016; Guo et al., 2017; Bai et al., 2018; Yuan and Yang, 2020; Chang et al., 2021; Du et al., 2021) and others were in English (Shi et al., 2013; Yang et al., 2013; Zhang et al., 2013; Gao et al., 2018; Gu et al., 2019; Khan et al., 2019; Liu et al., 2020; Rao et al., 2022). Figure 2 illustrates a flowchart of the study selection process.

3.2 Study quality

A modified 10-item CAMARADES checklist was used to assess the methodological quality of the included publications. Peer-reviewed articles were among the criteria; temperature management; construction of appropriate rodent models according to the study objectives; experimental animals were randomly assigned to treatment or control groups; blinded assessment of outcomes; explicit presentation of the use of anaesthetics without significant intrinsic neuroprotective activity; sample size calculations; compliance with animal welfare policies; and avoidance of potential conflicts of interest. All 24 articles used appropriate rodent models and reasonable groupings, all clearly reported sample sizes for each group and competing interests, and all were published in peer-reviewed publications. However, only 6 articles explicitly reported the use of anaesthetics with no apparent intrinsic neuroprotective activity, 4 did not mention temperature control in the experiments, 5 did not mention animal welfare policies, and no studies assessed outcomes blinded. The included articles' overall quality ratings ranged from 6 to 9. Two of the 24 articles received a score of 6 (8.33%), six received a score of 7 (25.00%), ten received a score of 8 (41.67%), and six received a score of 9 (25.00%). The methodological quality of each selected article is demonstrated in Figure 3.

3.3 Basic information and features of the articles included

The 24 papers had enough information to conduct a meta-analysis. These trials involved a total of 657 rodents, 330 of which were divided into the treatment group and the others were control group (Table 1).

Based on their biological traits, the animals used in the included researches were roughly categorized. The creatures were categorized into seven groups based on their species: 8.52% (56/657) Kunming

mice, 6.09% (40/657) ICR mice, 11.11% (73/657) C57BL/6 mice, 4.57% (30/657) BALB/c mice, 54.49% (358/657) Sprague Dawley Rats, 8.52% (56/657) Wistar rats and 6.70% (44/657) NIH mice. 63.01% (414/657) of rodents were rats, and 36.99% (243/657) of rodents were mice. The percentage of female and male rodents was 9.13% (60/657) and 87.21% (573/657) respectively regarding sex categorization, while 3.65% (24/657) of the rodents' sexes were unknown. Furthermore, according to the quality assessment scores, 25.00% (6/24) had 9 points, 41.67 (10/24) had 8 points, 25.00% (6/24) had 7 points, and 8.33% (2/24) had 6 points. Regarding the intervention time of MT, all experiments were divided into two subgroups: 76.10% (500/657) <4W groups and 23.90% (157/657) ≥4W groups. And the dosage of each experiment was divided into three groups: 24.96% (164/657) L-dosage groups, 23.14% (152/657) M-dosage group and 51.90% (341/657) H-dosage group (Supplementary Figure S1).

Across the studies, the weight of the animals included in the analysis varied from 17.7 g to 250 g, with a total number of examinations ranging from 10 to 184. The daily dosage of MT administered ranged from 2.8 mg/kg to 160 mg/kg, and the frequency of administration varied from a single dose to a maximum of 90 days.

3.4 Effects of MT on LI

The levels of ALT, AST, TNF- α and SOD which were the primary outcomes were assessed after MT therapy as well as the levels of MDA, IL-6, serum TG, serum TC and CAT were also changed by MT (Supplementary Tables S2, S3). Liver tissues from animals with LI exhibited significant inflammatory cell infiltration, hepatocyte swelling, vacuolar degeneration, and hepatocellular necrosis, as evidenced by H&E staining. The pathogenic alterations were significantly improved with MT treatment at dosage of 1.4–100 mg/kg, but the most effective dosage was the medium (25–50 mg/kg/d).

3.4.1 MT can improve the primary outcomes of LI

3.4.1.1 ALT levels

Because there was considerable heterogeneity ($I^2 > 50\%$), we performed a random-effects analysis. The findings revealed that the ALT levels were significantly reduced in the MT groups compared to the LI model groups ($n = 532$; 95% CI [-4.34, -2.50]; $SMD = |-3.42| > 1$; $I^2 = 90.30\%$; $p < 0.0001$) (Figure 4).

3.4.1.2 AST levels

The random-effect analysis was used for further analysis as the significant heterogeneity ($I^2 > 50\%$). The random-effect analysis revealed that the AST levels between the MT and LI model groups were significantly different. The levels of AST were shown to be reduced by MT ($n = 448$; 95% CI [-4.74, -2.78]; $SMD = |-3.76| > 1$; $I^2 = 87.50\%$; $p < 0.0001$) (Figure 4).

3.4.1.3 SOD levels

Significant heterogeneity ($I^2 > 50\%$) was observed, and a random-effects analysis was conducted. The results indicated that the amounts of SOD protein in the MT groups were substantially

greater than in the LI model groups ($n = 120$; 95% CI [2.66,5.33]; $SMD = |4.00| > 1$; $I^2 = 75.60\%$; $p < 0.0001$) (Figure 5).

3.4.1.4 MDA levels

The MDA levels in the mammalian models in the included study varied according to random-effects analyses. MDA levels in the MT groups were considerably lower than in the model groups ($n = 130$; 95% CI [-3.59, -1.81]; $SMD = |-2.70| > 1$; $I^2 = 64.40\%$; $p < 0.0001$) (Figure 5).

3.4.2 MT can administer the secondary outcomes of LI

3.4.2.1 Serum TG levels

The random-effects analysis showed that there were differences in serum TG levels between the MT and LI model groups. The MT groups had significantly lower levels of serum TG compared to the LI model group ($n = 100$; 95% CI [-2.70, -0.67]; $SMD = |-1.68| > 1$; $I^2 = 77.00\%$; $p = 0.001$) (Supplementary Figure S2).

3.4.2.2 Serum TC levels

In accordance with the random-effects analysis, the animal models in the included research had different serum TC levels. The MT groups had considerably lower serum TC levels than the model groups ($n = 88$; 95% CI [-2.59, -0.78]; $SMD = |-1.69| > 1$; $I^2 = 68.60\%$; $p < 0.0001$) (Supplementary Figure S2).

3.4.2.3 IL-6 levels

A random-effects analysis found notable IL-6 levels discrepancies between the MT and LI model groups. When compared to the LI model groups, IL-6 levels were substantially lower in the MT groups ($n = 254$; 95% CI [-4.87, -2.67]; $SMD = |-3.77| > 1$; $I^2 = 66.80\%$; $p < 0.0001$) (Supplementary Figure S3).

3.4.2.4 TNF- α levels

Because there was considerable heterogeneity ($I^2 > 50\%$), we performed a random-effects analysis for additional research. Regarding the random-effect analysis, the MT and LI model groups showed significantly different levels of TNF- α . TNF- α levels was observed to be reduced by MT ($n = 326$; 95% CI [-5.50, -1.95]; $SMD = |-3.72| > 1$; $I^2 = 94.60\%$; $p < 0.0001$) (Supplementary Figure S3).

3.4.2.5 CAT levels

The animal models in the included studies showed several differences between the MT and LI model groups in CAT levels, according to random-effect analysis. The MT groups had significantly higher levels of CAT than model groups ($n = 72$; 95% CI [2.23,3.62]; $SMD = |2.93| > 1$; $I^2 = 0.00\%$; $p < 0.0001$) (Supplementary Figure S3).

3.4.3 Subgroup analysis

3.4.3.1 Subgroup analysis of ALT levels

In comparison to the LI model groups, the levels of ALT were found to be significantly reduced in the MT groups. MT was effective in both rats ($n = 394$; 95% CI [-4.96, -2.44]; $SMD = |-3.70| > 1$; $I^2 = 92.20\%$; $p < 0.0001$) and mice ($n = 138$; 95% CI [-4.42, -1.67]; $SMD = |-3.05| > 1$; $I^2 = 85.90\%$; $p < 0.0001$) (Figure 4A1). The ALT levels were found to be reduced most by MT in the M-dosage subgroups ($n = 112$; 95% CI [-8.90, -2.86]; $SMD = |-5.88| > 1$;

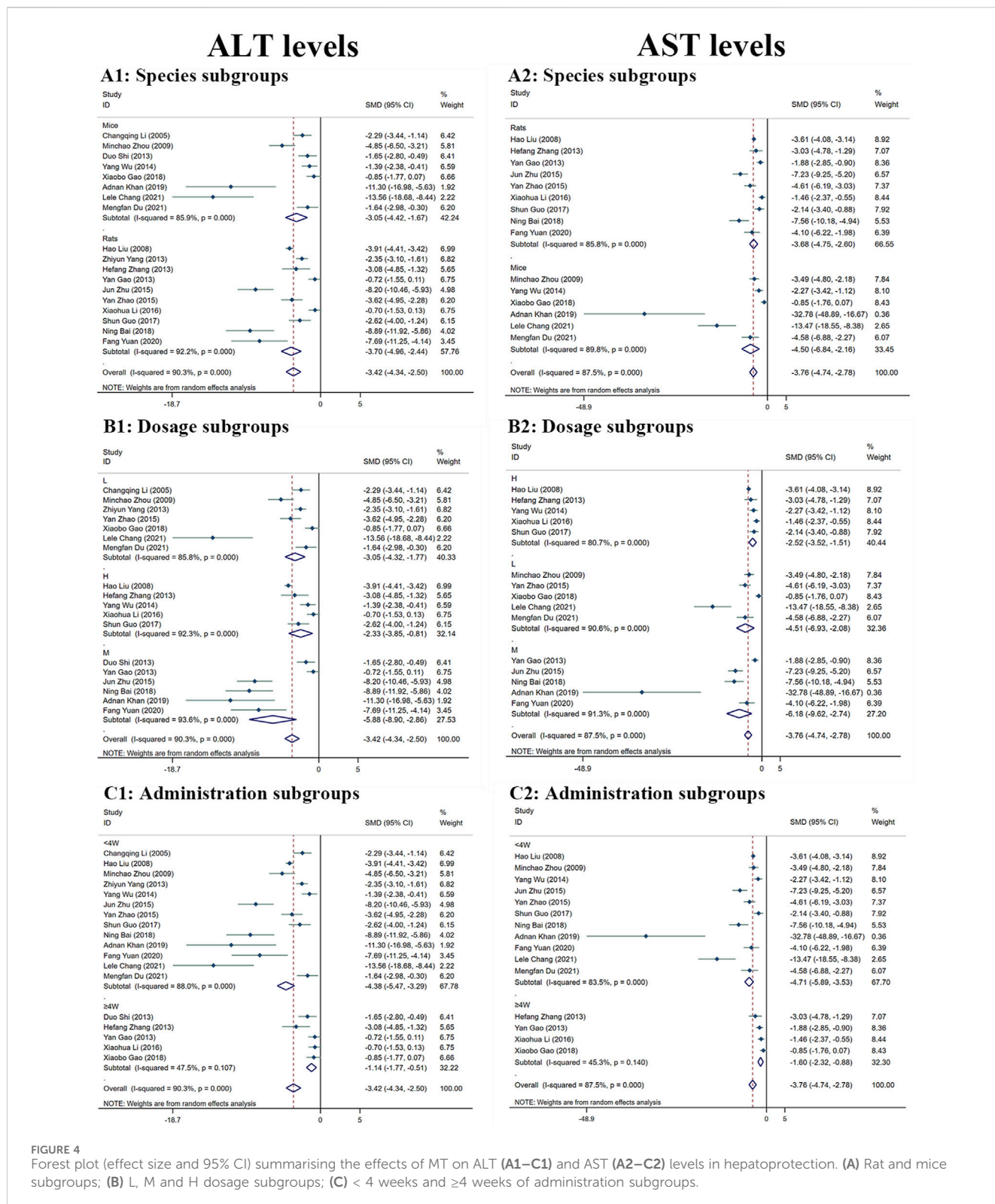


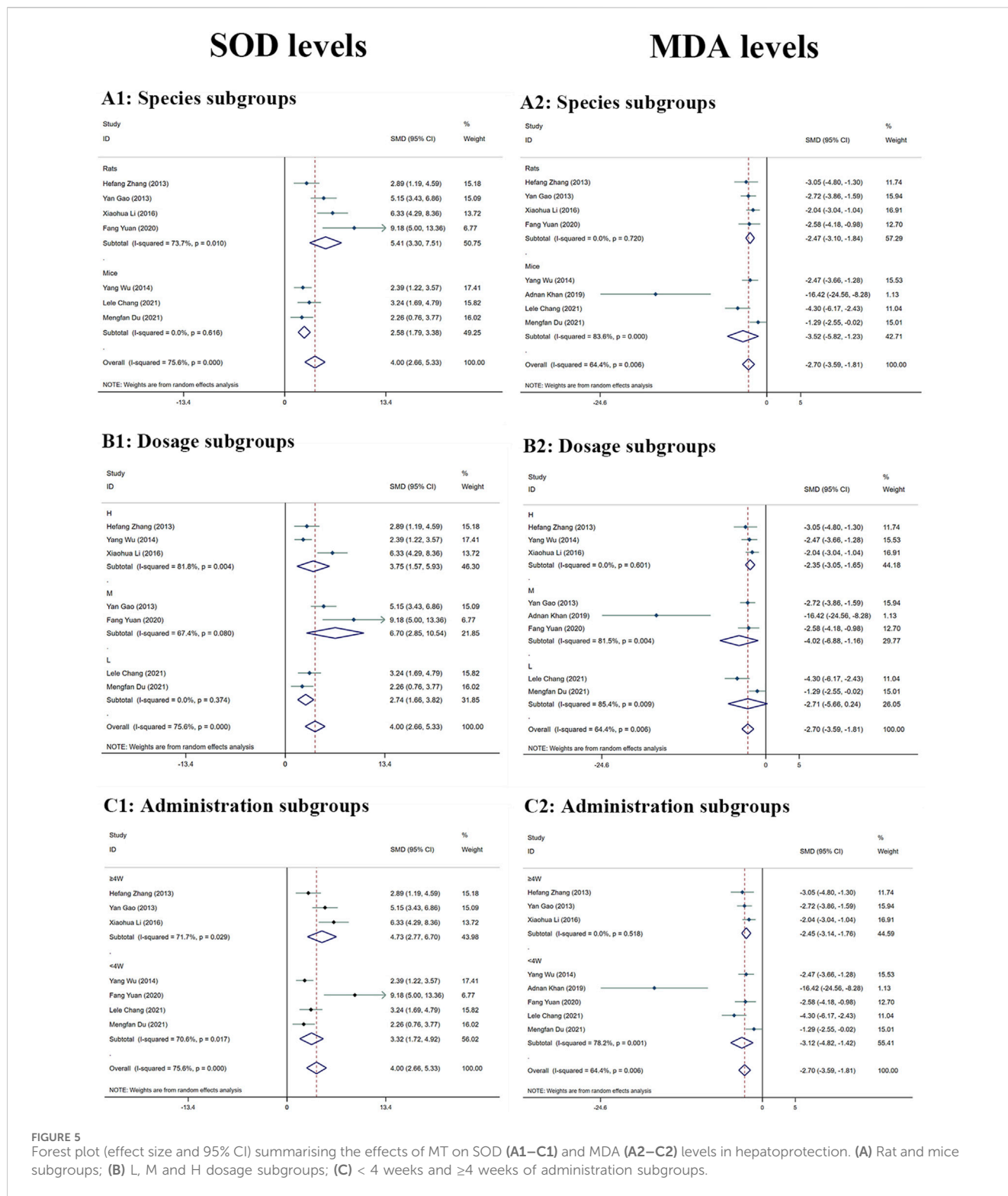
FIGURE 4 Forest plot (effect size and 95% CI) summarising the effects of MT on ALT (A1–C1) and AST (A2–C2) levels in hepatoprotection. (A) Rat and mice subgroups; (B) L, M and H dosage subgroups; (C) < 4 weeks and ≥4 weeks of administration subgroups.

$I^2 = 93.60\%$; $p < 0.0001$) than H-dosage ($n = 256$; 95% CI [-3.85, -0.81]; $SMD = |-2.33| > 1$; $I^2 = 92.30\%$; $p = 0.003$) and L-dosage subgroups ($n = 164$; 95% CI [-4.32, -1.77]; $SMD = |-3.05| > 1$; $I^2 = 85.80\%$; $p < 0.0001$) (Figure 4B1). Furthermore, it worked in both ‘≥4W’ subgroups ($n = 96$; 95% CI [-1.77, -0.51]; $SMD = |-1.14| > 1$; $I^2 = 47.50\%$; $p < 0.0001$) and ‘<4W’ subgroups ($n = 436$; 95% CI

[-5.47, -3.29]; $SMD = |-4.38| > 1$; $I^2 = 88.00\%$; $p < 0.0001$), but the lower levels were in the ‘<4W’ subgroups (Figure 4C1).

3.4.3.2 Subgroup analysis of AST levels

Compared with the LI model group, the levels of AST in MT groups were significantly lower. MT reduced substantially the AST



levels in both rats' subgroups (n = 346; 95% CI [-4.75, -2.60]; SMD = [-3.68] > 1; I² = 85.80%; p < 0.0001) and mice subgroups (n = 102; 95% CI [-6.84, -2.16]; SMD = [-4.50] > 1; I² = 89.80%; p < 0.0001) (Figure 4A2). MT had the most significant effect in the M-dosage subgroups (n = 96; 95% CI [-9.62, -2.74]; SMD = [-6.18] > 1; I² = 91.30%; p < 0.0001) than the other two subgroups (H-dosage subgroups: n = 256; 95% CI [-3.52, -1.51]; SMD = [-2.52] > 1; I² =

80.70%; p < 0.0001) (L-dosage subgroups: n = 96; 95% CI [-6.93, -2.08]; SMD = [-4.51] > 1; I² = 90.60%; p < 0.0001) (Figure 4B2). The levels of AST were decreased in the both two time-subgroups, but the lower groups were '<4W' subgroups ('≥4W' subgroups: n = 80; 95% CI [-2.32, -0.88]; SMD = [-1.60] > 1; I² = 45.30%; p < 0.0001) ('<4W' subgroups: n = 368; 95% CI [-5.89, -3.53]; SMD = [-4.71] > 1; I² = 83.50%; p < 0.0001) (Figure 4C2).

3.4.3.3 SOD levels subgroup analysis

The amount of SOD was significantly greater in the groups treated with MT than in the LI model groups. The levels of SOD were increased by MT in both rats subgroups ($n = 72$; 95% CI [3.30,7.51]; $SMD = |5.41| > 1$; $I^2 = 73.70\%$; $p < 0.0001$) and mice subgroups ($n = 48$; 95% CI [1.79,3.38]; $SMD = |2.58| > 1$; $I^2 = 0.00\%$; $p < 0.0001$) (Figure 5A1). The levels of SOD of M-dosage subgroups ($n = 36$; 95% CI [2.85,10.54]; $SMD = |6.70| > 1$; $I^2 = 67.40\%$; $p = 0.001$) were the highest by MT than H-dosage subgroups ($n = 56$; 95% CI [1.57,5.93]; $SMD = |3.75| > 1$; $I^2 = 81.80\%$; $p = 0.001$) and L-dosage subgroups ($n = 28$; 95% CI [1.66,3.82]; $SMD = |2.74| > 1$; $I^2 = 0.00\%$; $p < 0.0001$) (Figure 5B1). Furthermore, it worked in both '≥4W' subgroups ($n = 60$; 95% CI [2.77,6.70]; $SMD = |4.73| > 1$; $I^2 = 71.70\%$; $p < 0.0001$) and '<4W' subgroups ($n = 60$; 95% CI [1.72,4.92]; $SMD = |3.32| > 1$; $I^2 = 70.60\%$; $p < 0.0001$), but the higher levels were in the '<4W' subgroups (Figure 5C1).

3.4.3.4 Subgroup analysis of MDA levels

The MDA levels in the MT groups were lower than those in the LI model groups. The MDA levels were decreased by MT in both rats subgroups ($n = 72$; 95% CI [-3.10, -1.84]; $SMD = |-2.47| > 1$; $I^2 = 0.00\%$; $p < 0.0001$) and mice subgroups ($n = 58$; 95% CI [-5.82, -1.23]; $SMD = |-3.52| > 1$; $I^2 = 83.60\%$; $p = 0.003$) (Figure 5A2). MT reduced the MDA levels most in the M-dosage subgroups ($n = 46$; 95% CI [-2.55,-0.02]; $SMD = |-4.02| > 1$; $I^2 = 81.50\%$; $p = 0.006$) among the time subgroups (H-dosage subgroups: $n = 56$; 95% CI [-3.05,-1.65]; $SMD = |-2.35| > 1$; $I^2 = 0.00\%$; $p < 0.0001$) (L-dosage subgroups: $n = 28$; 95% CI [-5.66,0.24]; $SMD = |-4.51| > 1$; $I^2 = 85.40\%$; $p = 0.071$) (Figure 5B2). Moreover, it substantially lowered MDA levels in both '≥4W' subgroups ($n = 60$; 95% CI [-3.14, -1.76]; $SMD = |-2.45| > 1$; $I^2 = 0.00\%$; $p < 0.0001$) and '<4W' subgroups ($n = 70$; 95% CI [-4.82, -1.42]; $SMD = |-3.12| > 1$; $I^2 = 78.20\%$; $p < 0.0001$) (Figure 5C2).

3.4.4 Sensitivity analysis and publication bias of outcome indicators

The sensitivity of ALT, AST, SOD, and MDA levels in detecting LI in mouse models did not differ significantly. To identify publication bias, we used the |t|-value and conducted Egger's test. The |t|-values of these four factors did not indicate any publication bias in LI research (Supplementary Figures S4, S5).

3.5 The toxic effects of MT on liver

ALT and AST levels were examined as significant main indicators of toxic effects of MT on liver in five investigations. All the five investigations showed that MT can significantly increase ALT and AST levels. According to the results, MT may increase hepatotoxicity by influencing ALT and AST levels (Supplementary Table S4). H&E staining of normal animal liver tissues revealed significant hepatotoxicity with inflammatory cell infiltration, cell edema, cytoplasmic loosening and vacuolar degeneration of cytoplasm. Significant pathogenic alterations occurred with the intervention of MT at 10–69.1 mg/kg, but the most toxic dosage was the 30–62.5 mg/kg/d.

3.5.1 MT can affect the main indicators of liver function

3.5.1.1 ALT levels

Because of the considerable heterogeneity ($I^2 > 50\%$), the random-effects analysis was utilized for further investigation. The random-effects analysis revealed that the ALT levels between the MT and control groups were significantly different. The level of ALT was shown to be elevated by MT ($n = 105$; 95% CI [0.79, 3.02]; $SMD = |1.91| > 1$; $I^2 = 81.30\%$; $p < 0.0001$) (Figure 6A).

3.5.1.2 AST levels

The random-effect analysis revealed that the AST levels between the MT and control groups were significantly different. The level of AST was shown to be elevated by MT ($n = 105$; 95% CI [0.75, 3.68]; $SMD = |2.21| > 1$; $I^2 = 87.90\%$; $p < 0.0001$) (Figure 6B).

3.6 Dose–time–effect/dose–time–toxicity relationship

To achieve effective treatment for a disease, it is crucial to not only use the appropriate medications but also carefully consider the dosage and duration of drug administration. The three key elements in clinical treatment are identifying the most suitable medication, determining the ideal dosage, and establishing the optimal timing. In this study, we utilized three-dimensional mappings and radar charts to analyze the treatment duration and dosage in each research, aiming to identify the optimal length of treatment and dosage for MT that would yield the most effective results. Figures 7, 8 displayed 3D maps and radar charts corresponding to the four key indications.

3.6.1 The dose–time–effect/dose–time–toxicity relationship of ALT and AST levels

3.6.1.1 Effective dose and time length of MT on ALT and AST levels

The ALT and AST levels can be effectively reduced by MT in LI models at a dose of 1.4 mg/kg/d to 100 mg/kg/d, if all other conditions (except the dose of MT) are suitable. However, if the MT dose is less than 1.4 mg/kg/d or greater than 100 mg/kg/d, these effects are not observed. To ascertain the precise MT dosage that is effective, additional research are necessary. Considering the treatment period, 3D maps and radar charts indicate that MT effectively decrease ALT and AST levels at 0.02 W–4 W, but is unsuccessful in reducing these levels over 4.29 W. However, if the treatment period was 0.02W–0.86W at a medium dose (25–50 mg/kg/d), MT reduced ALT and AST levels more effectively than at a low dose (0–25 mg/kg/d) or a high dose (>50 mg/kg/d). Further study needs to be performed to determine the specific effective dose and administration of MT for a treatment duration of more than 4.29 W (Figures 7A,B; Figures 8A,B).

3.6.1.2 Toxic dose and time length of MT on ALT and AST levels

The levels of ALT and AST are increase by MT in normal models at a dosage of 10 mg/kg/d to 69.1 mg/kg/d, if all other conditions (except the dose of MT) are suitable. However, if the

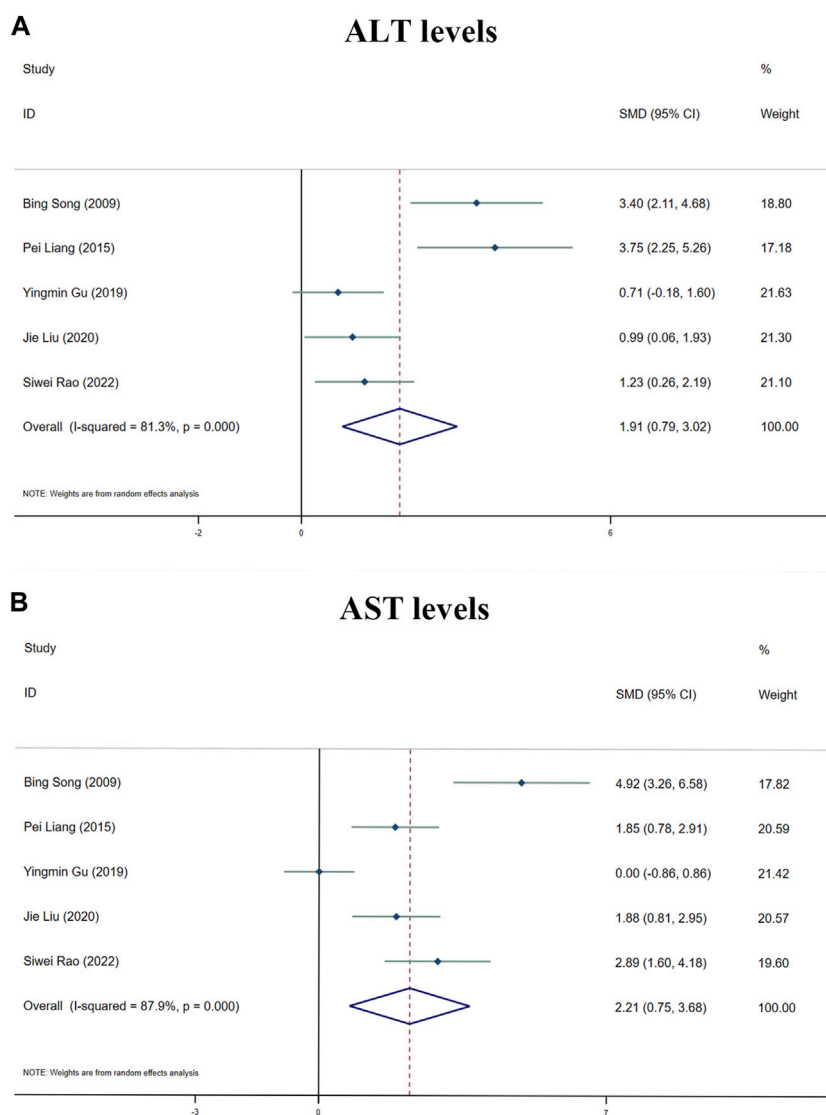


FIGURE 6 Forest plot (effect size and 95% CI) summarising the effects of MT on hepatotoxicity. **(A)** ALT levels; **(B)** AST levels.

MT dose is less than 10 mg/kg/d or greater than 100 mg/kg/d, the toxicity of MT is not observed. Considering the treatment period, 3D maps and radar charts indicate that MT effectively increase ALT and AST levels at 1W-2 W or 8.57W-12.86W, but is unknown at 2W-8.57W. Additional investigation needs to be conducted to study the specific toxic dose and administration of MT *in vivo* (Figures 7A,B; Figures 8A,B).

3.6.2 The impact of the effective dose and time length on SOD and MDA levels

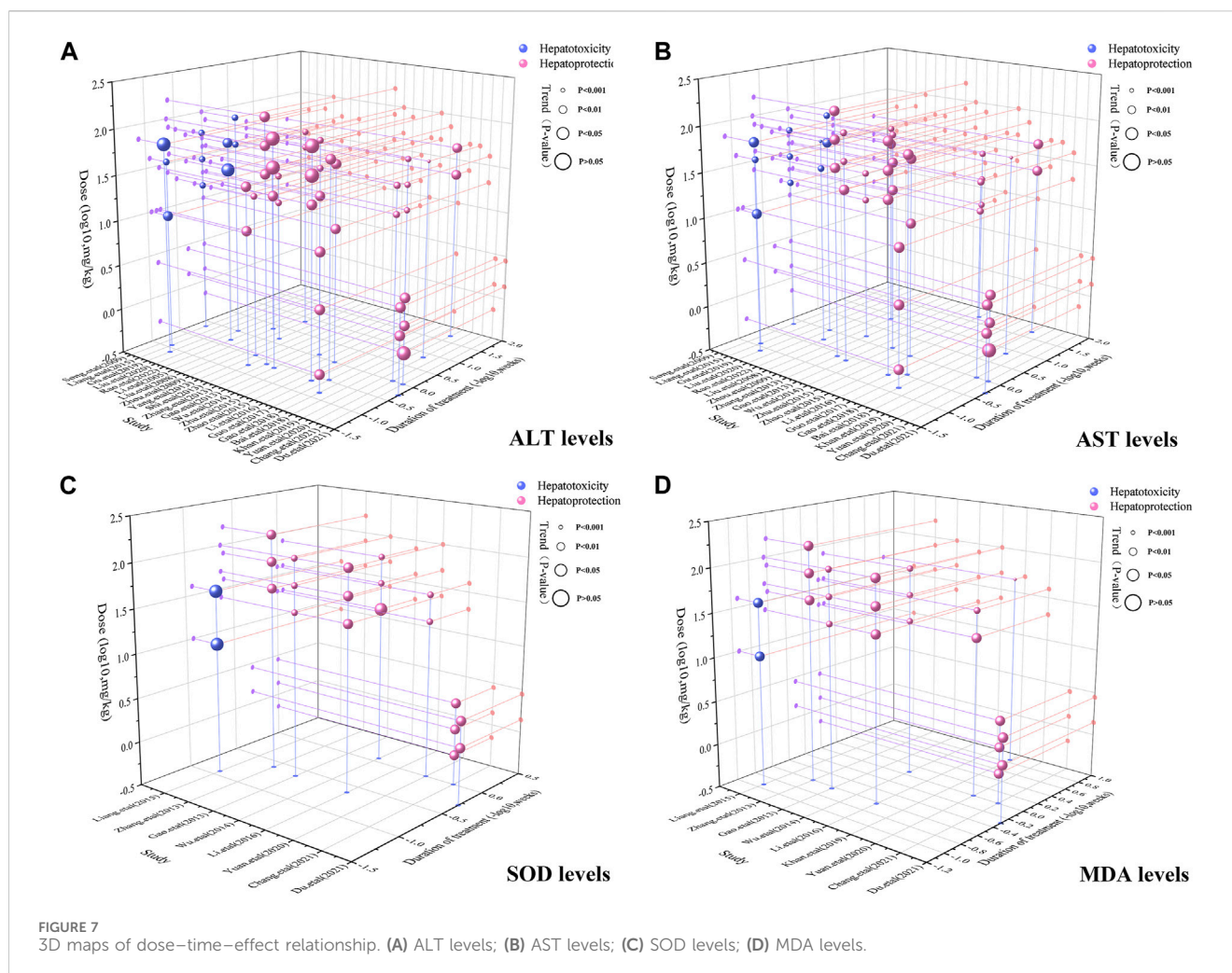
According to the 3D maps and radar charts, the SOD levels in the MT groups were higher than those in the LI model groups at a dose of 1.4 mg/kg/d to 100 mg/kg/d. At 1W-4.29W, MT was found to increase the amounts of SOD in the MT groups. MT, in contrast with MDA, can lower MDA levels at a dosage of 0.7 mg/kg/d to 100 mg/kg/d and a duration of 0.14 W-4.29 W (Figures 7C,D; Figures 8C,D).

3.7 Potential mechanisms of action of MT

The hypothesized bilateral impacts of MT on LI are extensive and complicated. The identified signalling transduction pathways, namely, SERCA, SREBP1c/SCAP, Notch/RBP-J/HES1, I κ K/NF- κ B, Cul3/Rbx1/Keap1/Nrf2, and Bcl-2/ROS/Bax/caspase-9/caspase-3 have been evaluated in Supplementary Tables S5-S6.

3.8 Molecular docking of key targets

To validate the potential mechanisms of action of MT, we utilized molecular docking to assess the binding affinity between MT and key targets. The molecular docking analysis demonstrated the interaction of MT with SERCA and SREBP-SCAP complexes, and the thermodynamic data was analyzed. The estimated free energy of -7.8 kcal/mol suggests that MT interacts with Phe256,



Phe834, Ile829, Ile765, Tyr837, Val769, Val263, and Met83 on the SERCA protein. Additionally, with an estimated free energy of -6.8 kcal/mol, MT exhibits significant interactions with Glu605, Leu647, Pro649, Trp690, Ala646, Ala602, Val688, Val603, and Ile645 on the SREBP-SCAP complexes. These interactions between MT and the targets involve beneficial patterns of hydrogen bonds and hydrophobic interactions. The compound–target interactions were visualized using PyMOL 2.6 and Discovery Studio 2019 (Figure 9).

4 Discussion

According to our meta-analysis, consisting of 24 published studies with 657 rodent models, MT provides information on liver protection and hepatotoxicity. We analyzed a range of indicators, such as TNF- α , IL-6, serum TG, serum TC, SOD, MDA, CAT, ALT, and AST, to establish the biological efficacy and diverse dosages of MT for treating and managing LI. Furthermore, by utilizing molecular docking techniques, we confirmed the interaction of MT with SERCA and SREBP-SCAP complexes, while also summarizing the mechanisms of MT as described in relevant literature. These findings aimed to gain a

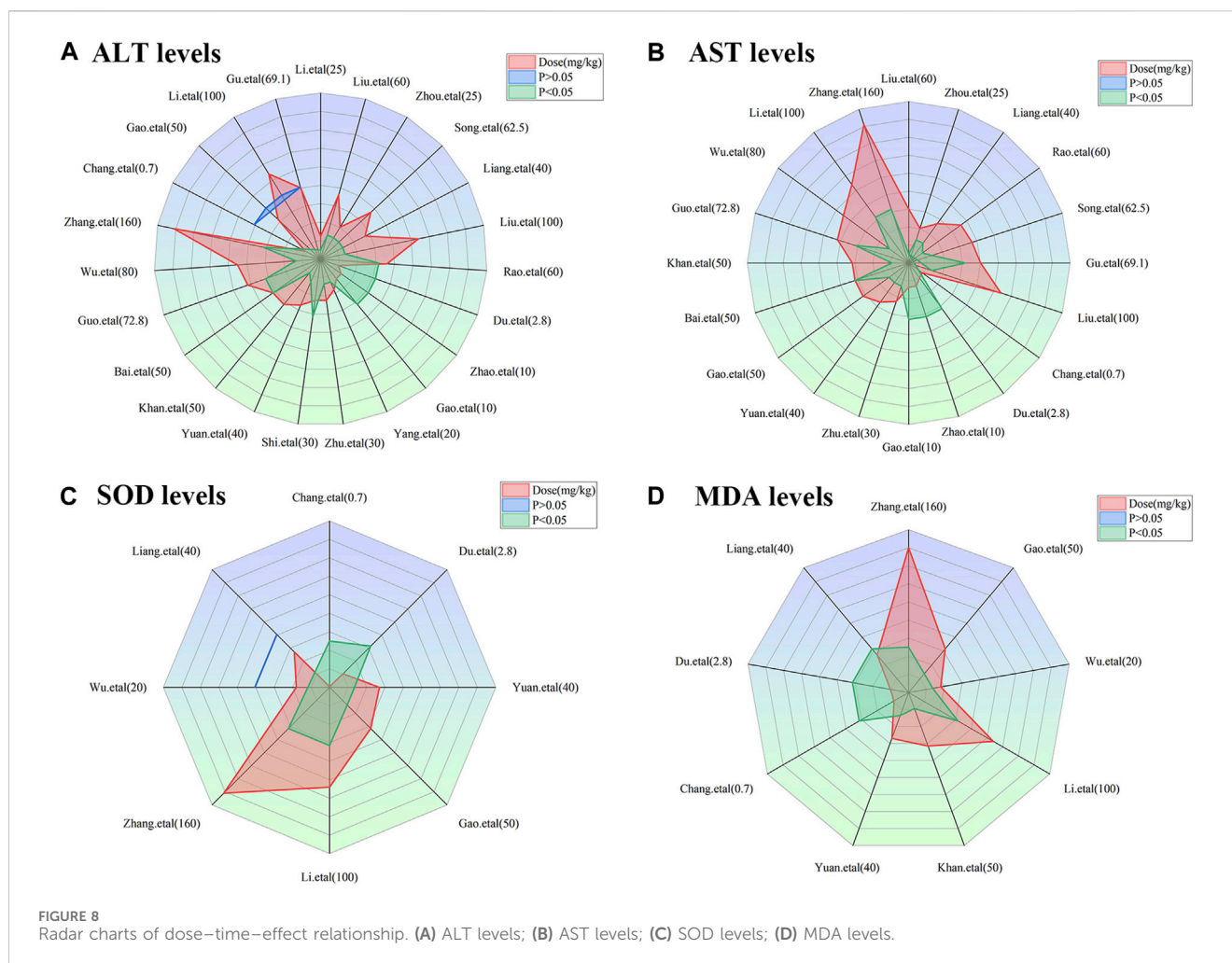
better understanding of the potential protective and harmful signaling pathways linked to the included indicators of MT on the LI (Figure 10).

4.1 The protective molecular mechanism of MT on LI

The comprehensive meta-analyses indicated that MT can protect from hepatotoxicity in animal models, and this protective effect is associated with variations in TNF- α , IL-6, serum TG, serum TC, MDA, ALT, AST, SOD, and CAT. Several signal transduction pathways are responsible for MT-induced alterations in these important indications of LI.

4.1.1 MT could inhibit SREBP1c in the LI models

Sterol regulatory element-binding protein-1c (SREBP1c), a transcription factor which is generated from ER, might have a critical function in the regulation of lipogenesis and be activated by different nutrient states in the liver (Sekiya et al., 2008). SREBPs and SREBP cleavage activating protein (SCAP) interact to form a complex on the endoplasmic reticulum membrane. When cells in mammals lack cholesterol, SREBP-SCAP complexes assemble

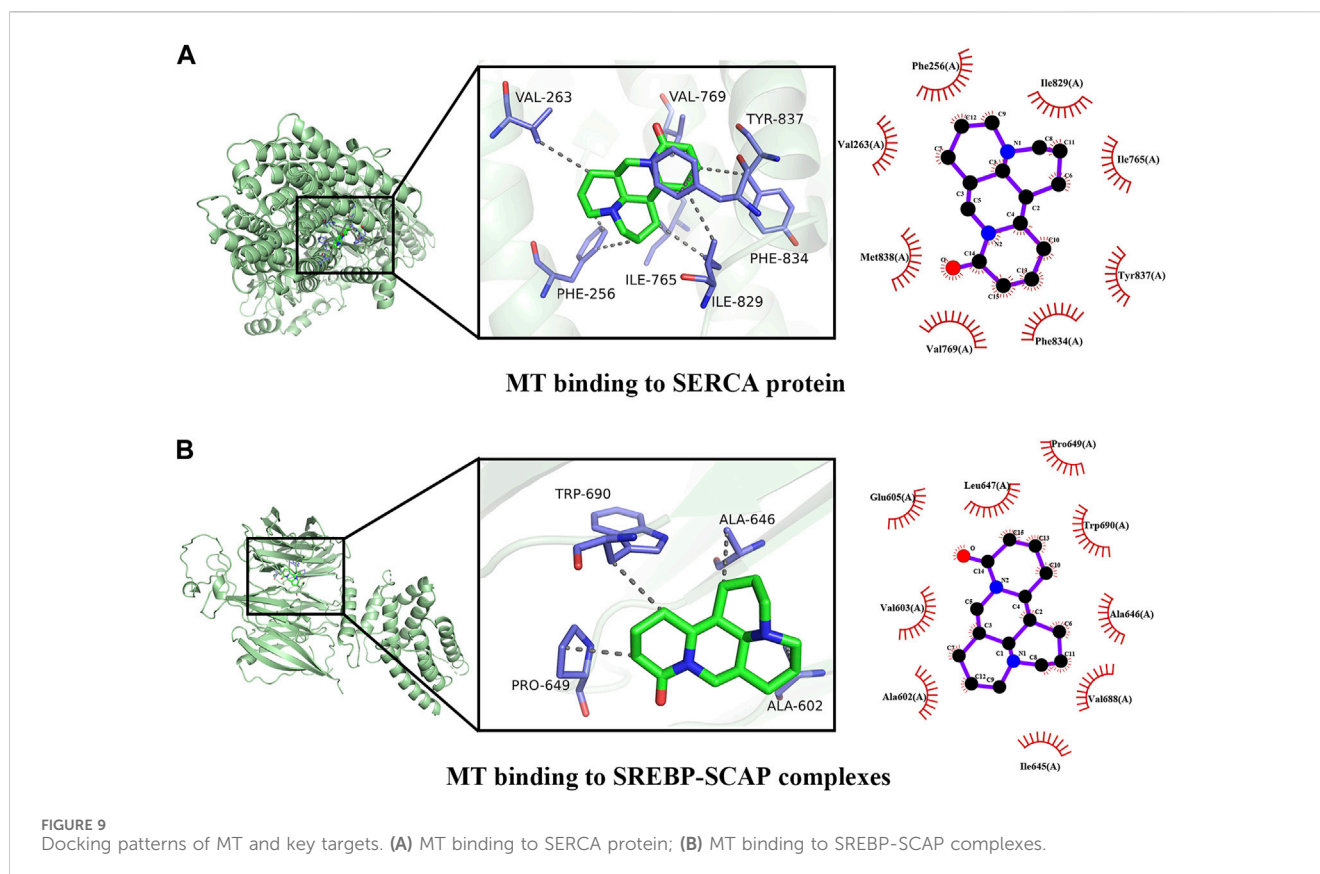


complexes in coat protein II (COPII) vesicles, facilitating transportation from the ER to the Golgi apparatus. To release the bHLH-Zip domains, SREBPs would be proteolyzed at the Golgi by site-1 and site-2 proteases (S1P and S2P) (Horton et al., 2002; Shimano and Sato, 2017; Lee et al., 2020). The translocated bHLH domain of SREBP1c interacts with the sterol regulatory element (SRE) in the nucleus, regulating the transcription of downstream lipid homeostasis genes such as fatty acid synthase (Fas), acetyl-CoA carboxylase (Acc), and stearoyl-CoA desaturase-1 (Scd1). SREBP1c also enhances the synthesis and accumulation of triacylglycerol (TG) in hepatocytes (Eberle et al., 2004). Previous studies have shown that the mechanistic target of rapamycin complex 1 mediates the nucleocytoplasmic transport of SREBP-1 and SREBP-2 (Peterson et al., 2011). A few findings indicate SREBP1c/2 may interact with NF- κ B to modulate inflammation and cholesterol stability (Fowler et al., 2022; Guo et al., 2017). NF- κ B enhances SCAP protein expression and promotes the activity of the SCAP-SREBP complex, which causes an inflammatory response and the accumulation of cholesterol (Lee et al., 2020; Li et al., 2013). In an animal model of nonalcoholic fatty liver disease (NAFLD) and nonalcoholic steatohepatitis (NASH) induced by a high-fat diet (HFD) or methionine-choline deficit (MCD), SREBP1c, Fas, Acc, ALT, AST, TNF- α , IL-6, and serum TC/TG levels are elevated. However, MT can reduce the levels of SREBP1c, Fas, Acc, ALT, AST,

TNF- α , and IL-6 in hepatocytes of HFD and MCD mice by decreasing SREBP1c expression (Rinella et al., 2008; Gao et al., 2018). Modulation of SREBP1c may be positively correlated with the production of liver damage indicators, and MT may have a potential impact on hepatic injury biomarkers (Yang et al., 2022).

4.1.2 MT might regulate Ca²⁺ homeostasis via SERCA to protect hepatocyte

Ca²⁺ is a second messenger that is required for cellular homeostasis through mTORC1, calmodulin, mitochondrial nitric oxide synthase, citric acid cycle (TCA cycle, Krebs cycle) and electron transport chain (ECT) and associated with ROS generation (Wan et al., 1989; O-Uchi et al., 2014; Jin et al., 2016; Tang et al., 2017; Diaz-Garcia et al., 2021; Stork et al., 2022). Extracellular stress stimuli such as CCL4, hepatic ischemia-reperfusion injury (HIRI), alcohol, and so on would increase Ca²⁺ transport from the extracellular area to the cytosol and mitochondria during the development of hepatic damage. The activation of Kupffer cells by hepatic I/R injuries is probably produced by the stimulation of store-operated Ca²⁺ channels (SOC), which increases Ca²⁺ influx into the cells and exacerbates the I/R-induced Kupffer cell injury (Pan et al., 2012). In rat liver, CCL4 might increase the expression and distribution of acid-sensing ion channel 1 (ASIC-1) (Pan et al., 2012). Consistent consumption of alcohol improves Ca²⁺-mediated



mitochondrial permeability transition pore opening and raises cyclophilin D levels within the liver (King et al., 2010).

A steady Ca^{2+} concentration gradient across the cell membrane is maintained by eukaryotic cells (~100 nM within the cytoplasm and ~1 mM extracellular milieu) (Bagur and Hajnoczky, 2017). The ER and mitochondria play essential roles in the storage, transport, and upkeep of Ca^{2+} within the cell. Ca^{2+} dysregulation in ER and mitochondria is associated with LI, including chronic viral hepatitis, alcoholic liver disease, and nonalcoholic fatty liver disease (Li et al., 2007; Mantena et al., 2008; King et al., 2010; Xiao et al., 2017). The connection between ER stress and lipid metabolism is linked to intracellular Ca^{2+} homeostasis in the liver. Recent accumulating investigations have connected Ca^{2+} concentration disruption to ER stress, proving to be a significant risk factor during the progression of NAFLD to NASH, leading to increased inositol-requiring enzyme 1 α (IRE1 α), activating transcription factor 6 α (ATF6 α), phosphoplasmic reticulum kinase (p-PERK), the 78 kDa glucose-regulated protein (GRP78), and C/EBP homologous protein (CHOP) expression (Bartlett et al., 2014; Park and Lee, 2014; Rieusset, 2017; Gao et al., 2018). Inactive GRP78, an ER chaperone protein, binds to three transmembrane unfolded protein response (UPR) stress sensors under physiological conditions: IRE1, ATF6 α , and PERK. When unfolding proteins assemble within the ER lumen, raising ER stress, GRP78 dissociates from these UPRs to capture the unfolding proteins and activate the UPR stress sensors.

ATF6 is transported from the ER to the Golgi apparatus once it has been separated from GRP78, where it can be cleaved by S1P and S2P. An activated form of ATF6 α might migrate to the nucleus and activate downstream target genes related to X-box-binding protein 1

(XBP1) and CHOP. ATF6 α signaling pathways may be able to alleviate ER stress. A serine-threonine kinase domain and an endoribonuclease domain have been identified in IRE1. The active IRE1 endonuclease activity could remove the introns of XBP1 mRNA to generate spliced XBP1 (sXBP1) mRNA. The sXBP1 protein functions as a transcription factor, translocating into the nucleus to stimulate the production of ER chaperones and the HSP40 family member P58^{IPK} gene. Activated PERK might cause dimerization and autophosphorylation of the kinase, allowing it to phosphorylate eukaryotic initiation factor 2 (eIF2). Phosphorylated eIF2 could block new protein translation while minimizing ER stress, hence assisting cell survival via transcription factor 4 (ATF4) activation. ATF4 could enter the nucleus and stimulate the production of the survival gene and the apoptotic cell death gene CHOP (Harding et al., 2003; Szegezdi et al., 2006).

Ca^{2+} is transported across the plasma membrane, the endoplasmic reticulum, and the mitochondria through Ca^{2+} channels. Prior studies have demonstrated that the sarco/endoplasmic reticulum Ca^{2+} -ATPase (SERCA) pump, a member of the P-type ATPase family of ion channels, transports intracellular Ca^{2+} from the cytosol to the ER and maintains Ca^{2+} homeostasis between the cytoplasm and ER lumen. Diminished SERCA activity could increase cytosolic Ca^{2+} level, ER stress, and apoptosis in NAFLD, whereas increased SERCA activity would reverse the process (Zhang et al., 2014; Lai et al., 2017). Lai et al. revealed that suppressing protein kinase C delta (PKC δ) could increase SERCA activity, thereby reducing ER stress (Lai et al., 2017). Meanwhile, Gao et al. demonstrated that exposing PA-induced

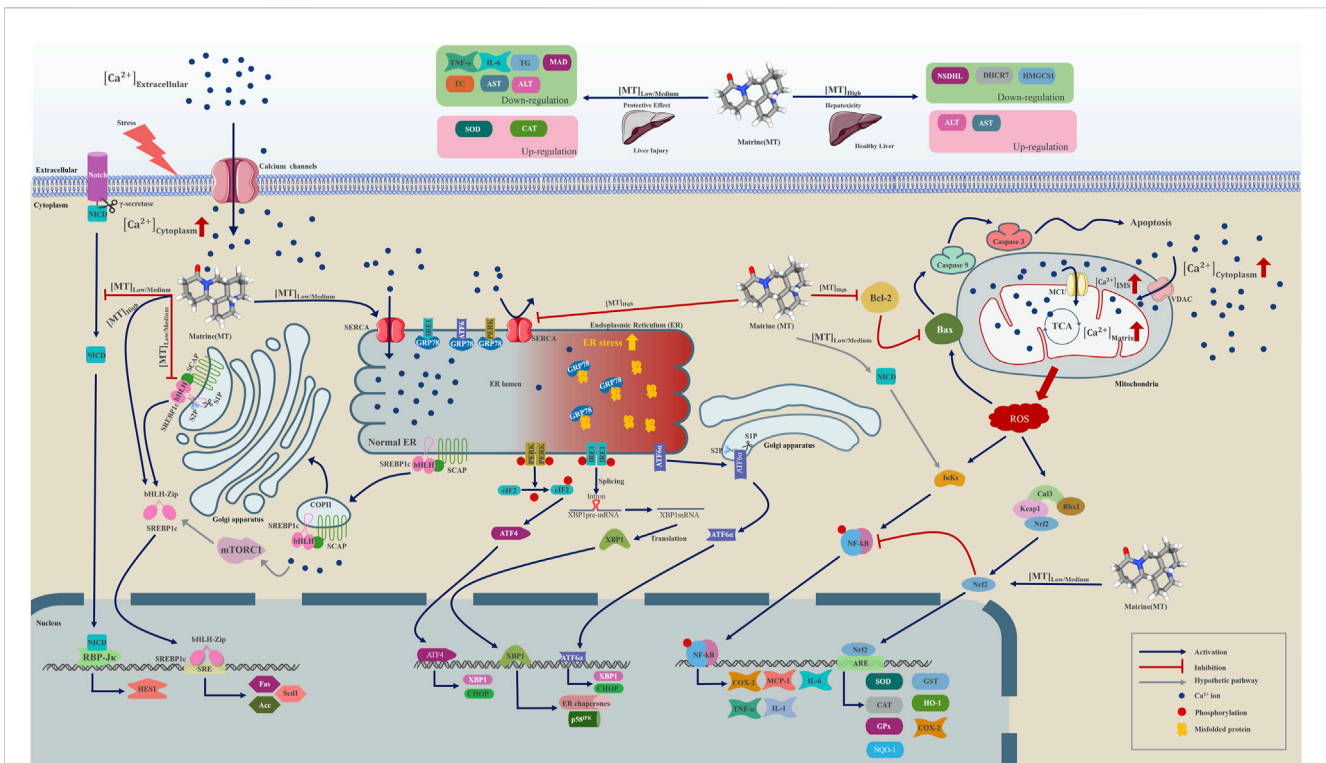


FIGURE 10
 A graphical representation illustrates multiple molecular processes of matrine protection and toxicity in liver injury by modifying SERCA, SREBP1c/SCAP, Notch/RBP-J/HES1, IK/NF- κ B, Cul3/Rbx1/Keap1/Nrf2, and Bcl-2/Bax/caspase 9/caspase 3 signalling pathways. Matrine probably plays a significant role in Ca²⁺ homeostasis regulation within the endoplasmic reticulum, Golgi apparatus, and mitochondria. Matrine could additionally influence the expression of three essential metabolically related genes, including DHCR7, NSDHL, and HMGCS1. Please check the abbreviation list.

L02 cells to low (200 μ M) and medium (400 μ M) doses of MT enhanced SERCA activity and facilitated Ca²⁺ influx from the cytosol into the ER lumen (Gao et al., 2018). These findings suggest that changes in SERCA function may contribute to the development of LI and provide a potential therapeutic target for various hepatic disorders.

4.1.3 MT would downregulate Notch/RBP-J/HES1 signaling cascade in the LI

Previous research found that inhibiting Notch signaling using RBP-J deletion or a Notch inhibitor worsened hepatic I/R damage, demonstrated by impaired liver function and increased hepatocyte apoptosis (Yu H. C. et al., 2011; Yue et al., 2018). The intracellular transmembrane domain (NICD) of the Notch receptor is released through the catalytic action of an integral membrane protein γ -secretase complex. NICD might enter the nucleus and bind the DNA-binding protein RBP-J, allowing Notch target genes such as HES1 to be transcribed. Earlier research proposed that MT may diminish HES1 mRNA levels by downregulating RBP-J κ mRNA expression to safeguard liver function and regeneration (Yang et al., 2013). The current study reveals that MT may promote hepatic progenitor cell development by obstructing the Notch/Jagged1/HES1 signaling pathway *in vivo* (Yang et al., 2016). By reducing SERCA activity and increasing ER stress in T-ALL cells, unmaturing Notch signaling transduction pathways would be activated, contributing to apoptosis (De Ford et al., 2016). We hypothesize that MT can suppress the Notch/RBP-J/

HES1 signaling cascade by promoting SERCA activity and minimize apoptosis in LI; however, more investigations are required.

4.1.4 MT might indirectly regulate NF- κ B activity via modifying SERCA in the LI

The nuclear factor kappa B (NF- κ B) is a recognized transcription factor in pro-inflammatory pathways. NF- κ B could potentially have an impact on controlling the processes of cell proliferation, differentiation, and cell death (Gerondakis et al., 2006; Khandelwal et al., 2011; Mitchell et al., 2016). TNF- α and IL-1, pro-inflammatory cytokines, may mediate NF- κ B signaling transduction pathways and encourage downstream target gene expression. NF- κ B activation will trigger the transcription and translation of COX-2, IL-6, MCP-1, TNF- α , and IL-1. The I κ B complex, which is composed of α and β subunits, is necessary for NF- κ B pathway activation via phosphorylation and ubiquitination. Previous literature has indicated that the activity of I κ B and NF- κ B is linked to various chronic liver injuries, including steatohepatitis, hepatocellular carcinoma, alcoholic liver disease, NAFLD, viral hepatitis, and biliary liver disease. Present results demonstrated that I κ B would interact with NICD directly to maintain the nuclear factor-kappa B (NF- κ B) activity in the T-ALL cells model (Vacca et al., 2006), and we proposed that MT therapeutic effect on Ca²⁺ ion channel SERCA might regulate the process of inflammation and apoptosis in the LI through NICD/NF- κ B interaction.

4.1.5 MT could increase Nrf2 translocation to nucleus and protective effect

Under normal state, nuclear factor erythroid 2-related factor 2 (Nrf2), as a protective molecule, could have a crucial function in preventing oxidation in the liver. In a physiological condition, Nrf2 might attach to the kelch-like ECH-associated protein 1 (Keap1), which is an adaptor to the E3 ubiquitin ligase complex Cullin3 (Cul3)/ring box protein 1 (Rbx1), and subsequently be ubiquitinated and suppressed by Cul3 in the cytoplasm. Recently research showed oxidative stress, the main pathologic feature of most liver diseases, could modify Keap1 and inhibit Nrf2 ubiquitination (Kobayashi et al., 2006; Saito et al., 2016). Nrf2 accumulation in the cytoplasm would translocate into the nucleus and bind to antioxidant-responsive elements (ARE) to transcript anti-oxidative and anti-inflammation genes expression involving superoxide dismutase (SOD), glutathione-S transferase (GST), glutathione peroxidase (GPx), catalase (CAT), heme oxygenase-1 (HO-1), quinone oxidoreductase-1 (NQO-1), and cyclooxygenase-2 (COX-2) (Pretera et al., 1995; Raghunath et al., 2018; Bardallo et al., 2022). Additionally, active Nrf2 may inhibit NF- κ Bp65 phosphorylation and reduce NF- κ Bp65 translocation to the nucleus in animal models to minimize inflammation and apoptosis. The PERK may collaborate with Nrf2 to improve cell survival after exposure to ER stress (Cullinan et al., 2003; Dai et al., 2018). We identified that MT could enhance the protective impact against hepatic damage via Nrf2 moving to the nucleus and activate downstream transcription of genes including CAT, SOD, and HO-1 in HFD-induced liver injury mouse models (Zhang et al., 2013).

4.2 The hepatotoxicity and molecular mechanism of MT on liver

As with the ER, mitochondria can potentially play an essential role in regulating Ca^{2+} homeostasis under physiological conditions. Specifically, Ca^{2+} could be transported to the outer membrane of mitochondria (OMM) through the voltage-dependent anion channels (VDACs) in the hepatocytes, and VDCAAs would be regulated by a series of proteins, including inositol 1,4,5-trisphosphate receptors (IP3Rs), ryanodine receptor (RyR), glucose-regulated protein 75 (GRP75), and sigma-1 receptor (S1R), to transfer Ca^{2+} into the intermembranous space (IMS). Elevated Ca^{2+} levels in the IMS could lead the mitochondrial Ca^{2+} uniporter (MCU) on the inner mitochondrial membrane (IMM) to interact with the mitochondrial Ca^{2+} uptake 1/2 (MICU1/2) and promote Ca^{2+} influx to the matrix (Hirata et al., 2002; Csordas et al., 2013; Williams et al., 2015; Shoshan-Barmatz et al., 2018). Furthermore, previous research has suggested that matrix Ca^{2+} can influence the cycle of TCA and the process of oxidative phosphorylation for ATP production. Interestingly, the required ROS might be created simultaneously in aerobic metabolism to maintain microdomain cell signaling (Bertero and Maack, 2018).

Gao et al. observed that excessive amounts of MT (800 μM) elevated SREBP1c, Fas, and Acc expression in PA-induced L02 cells. In comparison to low and medium dosages of MT, overdosage treatment results in the opposite effect. High-MT treatment causes toxicity and ultimately loss of protective capacity in the PA-induced L02 cell line (Gao et al., 2018). Furthermore, at low and medium levels, MT might have a therapeutic function of active SERCA to increase Ca^{2+} ion influx to the ER in response to stress, but excessive

MT would have a negative influence on this reaction. MT given in high doses inhibits SERCA activity, limiting Ca^{2+} transport from the cytosol to the ER lumen and increasing ER stress. Nonetheless, increased cytosolic Ca^{2+} may be transported across the mitochondria via VDACs, leading to a surge in Ca^{2+} accumulation within the IMS (Rapizzi et al., 2002; Shoshan-Barmatz et al., 2018). Ca^{2+} accumulation in the IMS stimulates the MCU to transport Ca^{2+} into the matrix. This process accelerates the metabolic rate of the TCA cycle and oxidative phosphorylation, resulting in an increase in mitochondrial ROS and apoptosis (Traaseth et al., 2004; Mallilankaraman et al., 2012; Csordas et al., 2013).

Overdosage of MT induces hepatotoxicity in animal models, and high-level MT may promote hepatocytes to produce higher ROS, increased HO-1, and the pro-apoptotic protein BAX while inhibiting the anti-apoptotic protein Bcl-2 synthesis. According to current research, mitochondrial ROS would activate NF- κ B, improve the production of inflammatory cytokines, and prevent Nrf2 degradation, hence increasing HO-1 expression (Wang et al., 2015; Lingappan, 2018; Kasai et al., 2020; Liu et al., 2020; Li et al., 2021). The present literature has demonstrated that raising cytosolic Ca^{2+} concentration could also activate the NF- κ B through elevating Ca^{2+} /Calmodulin-Dependent Protein Kinase II (CaMKII) activity to phosphorylate and degrade I κ K in the neurons (Snow and Albensi, 2016). Additionally, Rao et al. have discovered that MT-induced hepatotoxicity in the mice model suppresses three genes connected to steroid synthesis and metabolic processes in LI. These genes include 7-dehydrocholesterol reductase (DHCR7), NAD-(P)-dependent steroid dehydrogenase-like (NSDHL), and 3-hydroxy-3-methylglutaryl-coenzyme A synthase 1 (HMGCS1). However, the detailed mechanism is still to be further researched in the future (Rao et al., 2022).

4.3 The dual effects of matrine depend on dosage and molecular docking

The distinctive and dose-dependent effects of MT have been utilized to investigate various mechanisms of liver protection and hepatotoxicity. The suggested dosage, according to our data, is between 30–62.5 mg/kg/d, which can be harmful to rodent animal models. When given at a dosage of 20 mg/kg/d from 0.02W to 0.86W, MT demonstrated significant liver protection with no hepatotoxicity. Finally, our findings show that a dosage of 20–30 mg/kg/d of 0.02–0.86 W has a considerable liver-protective effect with low hepatotoxicity. A dosage of more than 30–62.5 mg/kg/d of MT therapy, on the other hand, caused liver damage in animal models. Through the activation of SERCA, SREBP-SCAP complexes, and MT, the pharmacological actions of MT can produce both liver protection and damage. These complexes are responsible for linking the IRE1, ATF6, and PERK proteins, all of which play important roles in regulating ER stress. The interaction of MT with SERCA and SREBP-SCAP complexes was demonstrated utilizing molecular docking, and the thermodynamic data was analyzed. With an estimated free energy of -7.8 kcal/mol, the molecule MT interacts with Phe256, Phe834, Ile829, Ile765, Tyr837, Val769, Val263, and Met83 on the SERCA protein.

With an estimated free energy of -6.8 kcal/mol, MT interacts substantially with the Glu605, Leu647, Pro649, Trp690, Ala646, Ala602, Val688, Val603, and Ile645 on the SREBP-SCAP complexes. SERCA and SREBP-SCAP complexes exhibit beneficial patterns of hydrogen bond and hydrophobic interactions.

4.4 Limitations

This meta-analysis adhered to the PRISMA standards (<http://prisma-statement.org/>), despite several limitations. 1) As only four English and four Chinese databases were utilized for article inclusion, selective bias was inevitable. In addition, we have not been able to compile all the relevant literature. 2) The heterogeneity of various studies could not be unified because of instrument index measurement error, different units of indicators, different experimental methods, etc. 3) Even though articles with quality scores of less than 5 points were disregarded, there may be heterogeneity in the results due to differences in the quality of the included articles. 4) The absence of a standardized method for animal intervention, drug dosage, treatment regimens, and model species across studies was another factor that might have caused the high heterogeneity. The reliability of MT's results in treating LI or causing hepatotoxicity was confirmed by the sensitivity analysis, Egger's test, and subgroup analysis. 5) Although the primary pharmacological mechanisms of MT in terms of liver protection and hepatotoxicity have been summarized, not all mechanisms could be summarized due to the complex pathogenic mechanisms involved. 6) The reliability of MT for hepatotoxicity may be lower than for hepatoprotection because only 5 articles on this condition were included. Future research should be conducted to investigate the hepatotoxicity of MT. 7) For ethical reasons, there is a paucity of literature on the toxicological effects of MT in the human body. Therefore, we only included studies using animal models. It is important to conduct relevant clinical trials to confirm the efficacy and reliability of MT in the clinical management of hepatoprotection and hepatotoxicity. 8) We validated the binding of MT to key proteins using molecular docking, but experiments were still needed to prove it.

Although this meta-analysis has several limitations, the findings may provide new strategies for clinical medication and drug development.

5 Conclusion

In summary, our study revealed that within the dose range of 10–69.1 mg/kg and time range of 1–2 weeks, MT could have a bilateral impact on liver damage. However, at a dose of 20–30 mg/kg/d for 0.02–0.86 weeks, it demonstrated high protection and low toxicity on the liver. Molecular docking analysis indicated that MT interacts with SERCA and SREBP-SCAP complexes. These interactions involve beneficial patterns of hydrogen bonds and hydrophobic interactions. By activating SERCA, a Ca^{2+} ion channel on the ER, MT could play a crucial role in regulating Ca^{2+} homeostasis in damaged hepatocytes. This helps maintain the balance among the cytoplasm, ER, Golgi apparatus, and mitochondria. Our findings suggest that MT doses ranging from 1.4 mg/kg/d to 100 mg/kg/d may have a

preventive and therapeutic effect on LI by modulating the expression of biomarkers such as TNF- α , IL-6, serum TG, serum TC, SOD, MDA, CAT, ALT, and AST. Additionally, signaling pathways such as SREBP1c/SCAP, Notch/RBP-J/HES1, I κ K/NF- κ B, and Cul3/Rbx1/Keap1/Nrf2 are likely involved in the protective process. It is interesting to note that many of these signaling pathways directly or indirectly interact with Ca^{2+} homeostasis. However, in normal hepatocytes, a high dosage of MT can suppress SERCA activity, leading to an adverse impact on Ca^{2+} homeostasis. This, in turn, can cause hepatotoxicity and promote apoptosis through the reduction of Bcl-2 and activation of the Ros/Bax/caspase 9/caspase 3 pathway. Elevated MT levels can also modulate the expression of various metabolic indicators, including AST, ALT, DHCR7, NSDHL, and HMGCS1. Further investigation is required to fully understand how MT influences the expression of these genes.

Data availability statement

The original contributions presented in the study are included in the article/[Supplementary Material](#), further inquiries can be directed to the corresponding authors.

Author contributions

WF: Conceptualization, Data curation, Methodology, Visualization, Writing–original draft. T-CK: Conceptualization, Data curation, Formal Analysis, Methodology, Visualization, Writing–original draft. JJ: Conceptualization, Data curation, Formal Analysis, Methodology, Visualization, Writing–original draft. XiZ: Data curation, Visualization, Writing–original draft. SC: Data curation, Visualization, Writing–original draft. JZ: Conceptualization, Writing–review and editing. YC: Conceptualization, Writing–review and editing. XM: Conceptualization, Writing–review and editing.

Funding

The author(s) declare financial support was received for the research, authorship, and/or publication of this article. This work was supported by Sichuan Science and Technology Program (2023NSFSC0687), Xinglin Scholar Research Promotion Project of Chengdu University of TCM (grant nos. QJRC2022028 and QJJ2022010), Major scientific research problems and key topics of medical technology problems of China Medical Education Association (2022KTZ016) and “The Hundred Talents Program” of the Hospital of the Chengdu University of Traditional Chinese Medicine (grant no. 22- B09).

Acknowledgments

This paper has been greatly improved by the advice of the reviewers and the authors of all references. The authors wish to thank the reviewers and the authors of all references.

Conflict of interest

The authors declare that the research was conducted in the absence of any commercial or financial relationships that could be construed as a potential conflict of interest.

Publisher's note

All claims expressed in this article are solely those of the authors and do not necessarily represent those of their affiliated

organizations, or those of the publisher, the editors and the reviewers. Any product that may be evaluated in this article, or claim that may be made by its manufacturer, is not guaranteed or endorsed by the publisher.

Supplementary material

The Supplementary Material for this article can be found online at: <https://www.frontiersin.org/articles/10.3389/fphar.2024.1315584/full#supplementary-material>

References

- Bagur, R., and Hajnoczky, G. (2017). Intracellular Ca(2+) sensing: its role in calcium homeostasis and signaling. *Mol. Cell* 66 (6), 780–788. doi:10.1016/j.molcel.2017.05.028
- Bai, N., Wang, D., Ouyang, X., Zhou, L., and Wang, Z. (2018). Inhibitory effect of matrine against hepatic ischemia-reperfusion injury in rats and its mechanism. *Chin. J. General Surg.* 27, 81–86. doi:10.3978/j.issn.1005-6947.2018.01.013
- Bardallo, R. G., Panisello-Rosello, A., Sanchez-Nuno, S., Alva, N., Rosello-Catafau, J., and Carbonell, T. (2022). Nrf2 and oxidative stress in liver ischemia/reperfusion injury. *FEBS J.* 289 (18), 5463–5479. doi:10.1111/febs.16336
- Bartlett, P. J., Gaspers, L. D., Pierobon, N., and Thomas, A. P. (2014). Calcium-dependent regulation of glucose homeostasis in the liver. *Cell Calcium* 55 (6), 306–316. doi:10.1016/j.ceca.2014.02.007
- Bertero, E., and Maack, C. (2018). Calcium signaling and reactive oxygen species in mitochondria. *Circ. Res.* 122 (10), 1460–1478. doi:10.1161/CIRCRESAHA.118.310082
- Chang, L., Wang, S., Dou, L., Jia, M., Wang, T., and Xu, B. (2021). Protective mechanism of matrine against liver injury induced by acetaminophen in mice. *China J. Mod. Med.* 31, 58–63. doi:10.3969/j.issn.1005-8982.2021.19.011
- Chemaly, E. R., Troncone, L., and Lebeche, D. (2018). SERCA control of cell death and survival. *Cell Calcium* 69, 46–61. doi:10.1016/j.ceca.2017.07.001
- Chinese Pharmacopoeia Commission (2020). *The Pharmacopoeia of the people's Republic of China, 2020*. ed. Part I. Beijing, China: China Medical Science Press, 211.
- Chu, Y., Jing, Y., Zhao, X., Wang, M., Zhang, M., Ma, R., et al. (2021). Modulation of the HMGB1/TLR4/NF- κ B signaling pathway in the CNS by matrine in experimental autoimmune encephalomyelitis. *J. Neuroimmunol.* 352, 577480. doi:10.1016/j.jneuroim.2021.577480
- Csordas, G., Golenar, T., Seifert, E. L., Kamer, K. J., Sancak, Y., Perocchi, F., et al. (2013). MICU1 controls both the threshold and cooperative activation of the mitochondrial Ca²⁺ uniporter. *Cell Metab.* 17 (6), 976–987. doi:10.1016/j.cmet.2013.04.020
- Cullinan, S. B., Zhang, D., Hannink, M., Arvais, E., Kaufman, R. J., and Diehl, J. A. (2003). Nrf2 is a direct PERK substrate and effector of PERK-dependent cell survival. *Mol. Cell Biol.* 23 (20), 7198–7209. doi:10.1128/MCB.23.20.7198-7209.2003
- Dai, Y., Zhang, H., Zhang, J., and Yan, M. (2018). Isoquercetin attenuates oxidative stress and neuronal apoptosis after ischemia/reperfusion injury via Nrf2-mediated inhibition of the NOX4/ROS/NF- κ B pathway. *Chem. Biol. Interact.* 284, 32–40. doi:10.1016/j.cbi.2018.02.017
- De Ford, C., Heidersdorf, B., Haun, F., Murillo, R., Friedrich, T., Borner, C., et al. (2016). The clerodane diterpene casearin J induces apoptosis of T-ALL cells through SERCA inhibition, oxidative stress, and interference with Notch1 signaling. *Cell Death Dis.* 7 (1), e2070. doi:10.1038/cddis.2015.413
- Devarbhavi, H., Asrani, S. K., Arab, J. P., Nartey, Y. A., Pose, E., and Kamath, P. S. (2023). Global burden of liver disease: 2023 update. *J. Hepatol.* 79 (2), 516–537. doi:10.1016/j.jhep.2023.03.017
- Diaz-Garcia, C. M., Meyer, D. J., Nathwani, N., Rahman, M., Martinez-Francois, J. R., and Yellen, G. (2021). The distinct roles of calcium in rapid control of neuronal glycolysis and the tricarboxylic acid cycle. *Elife* 10, e64821. doi:10.7554/eLife.64821
- Du, M., Xu, B., Xiang, R., Guo, D., Fan, Y., Shi, X., et al. (2021). The protective effect of Matrine injection on acute alcoholic liver injury in mice. *China J. Mod. Med.* 31, 13–18. doi:10.3969/j.issn.1005-8982.2021.24.003
- Eberle, D., Hegarty, B., Bossard, P., Ferre, P., and Foulle, F. (2004). SREBP transcription factors: master regulators of lipid homeostasis. *Biochimie* 86 (11), 839–848. doi:10.1016/j.biochi.2004.09.018
- Fowler, J. W. M., Zhang, R., Tao, B., Boutagy, N. E., and Sessa, W. C. (2022). Inflammatory stress signaling via NF- κ B alters accessible cholesterol to upregulate SREBP2 transcriptional activity in endothelial cells. *Elife* 86 (11). doi:10.7554/eLife.79529
- Gao, X., Guo, S., Zhang, S., Liu, A., Shi, L., and Zhang, Y. (2018). Matrine attenuates endoplasmic reticulum stress and mitochondrion dysfunction in nonalcoholic fatty liver disease by regulating SERCA pathway. *J. Transl. Med.* 16 (1), 319. doi:10.1186/s12967-018-1685-2
- Gao, X., Guo, S., Zhang, S., Liu, A., Shi, L., and Zhang, Y. (2019). Correction to: matrine attenuates endoplasmic reticulum stress and mitochondrion dysfunction in nonalcoholic fatty liver disease by regulating SERCA pathway. *J. Transl. Med.* 17 (1), 277. doi:10.1186/s12967-019-2020-2
- Gao, Y., Zheng, P., Yan, L., and Dai, G. (2013). Preliminary mechanism study of matrine on chronic alcohol-induced hepatic injury in rats. *Chin. Pharmacol. Bull.* 29, 1012–1016. doi:10.3969/j.issn.1001-1978.2013.07.028
- Gerondakis, S., Grumont, R., Gugasyan, R., Wong, L., Isomura, I., Ho, W., et al. (2006). Unravelling the complexities of the NF- κ B signalling pathway using mouse knockout and transgenic models. *Oncogene* 25 (51), 6781–6799. doi:10.1038/sj.onc.1209944
- Gu, Y., Lu, J., Sun, W., Jin, R., Ohira, T., Zhang, Z., et al. (2019). Oxymatrine and its metabolite matrine contribute to the hepatotoxicity induced by radix Sophorae tonkinensis in mice. *Exp. Ther. Med.* 17 (4), 2519–2528. doi:10.3892/etm.2019.7237
- Guo, S., Zhang, S., Wei, H., Shi, L., Hu, N., Dang, X., et al. (2017). Protective effect and mechanism of matrine combined with glycyrrhizic acid in the treatment of chronic liver injury induced by carbon tetrachloride. *China Pharm.* 20, 1153–1158.
- Harding, H. P., Zhang, Y., Zeng, H., Novoa, I., Lu, P. D., Calton, M., et al. (2003). An integrated stress response regulates amino acid metabolism and resistance to oxidative stress. *Mol. Cell* 11 (3), 619–633. doi:10.1016/s1097-2765(03)00105-9
- He, X., Fang, J., Huang, L., Wang, J., and Huang, X. (2015). *Sophora flavescens* Ait.: traditional usage, phytochemistry and pharmacology of an important traditional Chinese medicine. *J. Ethnopharmacol.* 172, 10–29. doi:10.1016/j.jep.2015.06.010
- Hirata, K., Pusch, T., O'Neill, A. F., Dranoff, J. A., and Nathanson, M. H. (2002). The type II inositol 1,4,5-trisphosphate receptor can trigger Ca²⁺ waves in rat hepatocytes. *Gastroenterology* 122 (4), 1088–1100. doi:10.1053/gast.2002.32363
- Horton, J. D., Goldstein, J. L., and Brown, M. S. (2002). SREBPs: activators of the complete program of cholesterol and fatty acid synthesis in the liver. *J. Clin. Investigation* 109 (9), 1125–1131. doi:10.1172/JCI15593
- Jin, Y., Bai, Y., Ni, H., Qiang, L., Ye, L., Shan, Y., et al. (2016). Activation of autophagy through calcium-dependent AMPK/mTOR and PKC θ pathway causes activation of rat hepatic stellate cells under hypoxic stress. *FEBS Lett.* 590 (5), 672–682. doi:10.1002/1873-3468.12090
- Jing, Y., Ma, R., Chu, Y., Dou, M., Wang, M., Li, X., et al. (2021). Matrine treatment induced an A2 astrocyte phenotype and protected the blood-brain barrier in CNS autoimmunity. *J. Chem. Neuroanat.* 117, 102004. doi:10.1016/j.jchemneu.2021.102004
- Ju, J., Li, J., Lin, Q., and Xu, H. (2018). Efficacy and safety of berberine for dyslipidaemias: a systematic review and meta-analysis of randomized clinical trials. *Phytomedicine* 50, 25–34. doi:10.1016/j.phymed.2018.09.212
- Kasai, S., Shimizu, S., Tataru, Y., Mimura, J., and Itoh, K. (2020). Regulation of Nrf2 by mitochondrial reactive oxygen species in physiology and pathology. *Biomolecules* 10 (2), 320. doi:10.3390/biom10020320
- Kaufman, R. J., and Malhotra, J. D. (2014). Calcium trafficking integrates endoplasmic reticulum function with mitochondrial bioenergetics. *Biochim. Biophys. Acta* 1843 (10), 2233–2239. doi:10.1016/j.bbamcr.2014.03.022
- Khan, A., Shal, B., Naveed, M., Shah, F. A., Atiq, A., Khan, N. U., et al. (2019). Matrine ameliorates anxiety and depression-like behaviour by targeting hyperammonemia-induced neuroinflammation and oxidative stress in CCl4 model of liver injury. *Neurotoxicology* 72, 38–50. doi:10.1016/j.neuro.2019.02.002
- Khandelwal, N., Simpson, J., Taylor, G., Rafique, S., Whitehouse, A., Hiscox, J., et al. (2011). Nucleolar NF- κ B/RelA mediates apoptosis by causing cytoplasmic relocalization of nucleophosmin. *Cell Death Differ.* 18 (12), 1889–1903. doi:10.1038/cdd.2011.79

- King, A. L., Swain, T. M., Dickinson, D. A., Lesort, M. J., and Bailey, S. M. (2010). Chronic ethanol consumption enhances sensitivity to Ca²⁺-mediated opening of the mitochondrial permeability transition pore and increases cyclophilin D in liver. *Am. J. Physiol. Gastrointest. Liver Physiol.* 299 (4), G954–G966. doi:10.1152/ajpgi.00246.2010
- Knight, J. A. (2005). Liver function tests: their role in the diagnosis of hepatobiliary diseases. *J. Infus. Nurs.* 28 (2), 108–117. doi:10.1097/00129804-200503000-00004
- Kobayashi, A., Kang, M. I., Watai, Y., Tong, K. I., Shibata, T., Uchida, K., et al. (2006). Oxidative and electrophilic stresses activate Nrf2 through inhibition of ubiquitination activity of Keap1. *Mol. Cell Biol.* 26 (1), 221–229. doi:10.1128/MCB.26.1.221-229.2006
- Lai, S., Li, Y., Kuang, Y., Cui, H., Yang, Y., Sun, W., et al. (2017). PKC δ silencing alleviates saturated fatty acid induced ER stress by enhancing SERCA activity. *Biosci. Rep.* 37 (6). doi:10.1042/BSR20170869
- Lee, S. H., Lee, J. H., and Im, S. S. (2020). The cellular function of SCAP in metabolic signaling. *Exp. Mol. Med.* 52 (5), 724–729. doi:10.1038/s12276-020-0430-0
- Li, L. C., Varghese, Z., Moorhead, J. F., Lee, C. T., Chen, J. B., and Ruan, X. Z. (2013). Cross-talk between TLR4-MyD88-NF- κ B and SCAP-SREBP2 pathways mediates macrophage foam cell formation. *Am J. Physiol. Heart Circ. Physiol.* 304 (6), H874–H884. doi:10.1152/ajpheart.00096.2012
- Li, C., Liu, L., Mo, C., and Huang, L. (2005). Effects of Matrine on release of interferon and pathological changes in concanavalin A-induced liver injury in mice. *World Chin. J. Dig.* 13, 640–643.
- Li, D., Hong, X., Zhao, F., Ci, X., and Zhang, S. (2021). Targeting Nrf2 may reverse the drug resistance in ovarian cancer. *Cancer Cell Int.* 21 (1), 116. doi:10.1186/s12935-021-01822-1
- Li, X., Cheng, G., and Zhou, F. (2016). The effects of matrine on blood lipids and antioxidant capacity in rats with chronic alcoholic liver injury. *Chin. J. Geriatrics* 36, 1838–1839. doi:10.3969/j.issn.1005-9202.2016.08.021
- Li, Y., Boehning, D. F., Qian, T., Popov, V. L., and Weinman, S. A. (2007). Hepatitis C virus core protein increases mitochondrial ROS production by stimulation of Ca²⁺ uniporter activity. *FASEB J.* 21 (10), 2474–2485. doi:10.1096/fj.06-7345com
- Liang, P., Yuan, T., Gu, L., and Lu, H. (2015). Study of hepatotoxicity and neural behavioral changes of *Sophora flavescens* and matrine in mice. *Chin. J. Mod. Appl. Pharm.* 32, 1444–1448. doi:10.13748/j.cnki.issn1007-7693.2015.12.008
- Lingappan, K. (2018). NF- κ B in oxidative stress. *Curr. Opin. Toxicol.* 7, 81–86. doi:10.1016/j.cotox.2017.11.002
- Liu, H., Qiu, Y., Mao, L., Zhu, X., and Ding, Y. (2008). Protective effect of matrine against ischemia and reperfusion injury in rat partial liver transplantation. *World Chin. J. Dig.* 16, 1617–1621. doi:10.11569/wjcd.v16.i15.1617
- Liu, J., Zhao, Y., Xia, J., and Qiu, M. (2020). Matrine induces toxicity in mouse liver cells through an ROS-dependent mechanism. *Res. Vet. Sci.* 132, 308–311. doi:10.1016/j.rvsc.2020.07.006
- Liu, M., Pu, Y., Gu, J., He, Q., Liu, Y., Zeng, Y., et al. (2021). Evaluation of Zhilong Huoxue Tongyu capsule in the treatment of acute cerebral infarction: a systematic review and meta-analysis of randomized controlled trials. *Phytomedicine* 86, 153566. doi:10.1016/j.phymed.2021.153566
- Liu, Q., and Zhang, X. S. (2021). Analysis of clinical application literature on matrine injection. *Chin. Jof Clin. Ration. Drug Use* 14, 12A. doi:10.15887/j.cnki.13-1389/r.2021.34.072
- Luo, X., Ni, X., Lin, J., Zhang, Y., Wu, L., Huang, D., et al. (2021). The add-on effect of Chinese herbal medicine on COVID-19: a systematic review and meta-analysis. *Phytomedicine* 85, 153282. doi:10.1016/j.phymed.2020.153282
- Macleod, M. R., O'Collins, T., Howells, D. W., and Donnan, G. A. (2004). Pooling of animal experimental data reveals influence of study design and publication bias. *Stroke* 35 (5), 1203–1208. doi:10.1161/01.Str.0000125719.25853.20
- Mallilankaraman, K., Doonan, P., Cardenas, C., Chandramoorthy, H. C., Muller, M., Miller, R., et al. (2012). MICU1 is an essential gatekeeper for MCU-mediated mitochondrial Ca²⁺ uptake that regulates cell survival. *Cell* 151 (3), 630–644. doi:10.1016/j.cell.2012.10.011
- Mantena, S. K., King, A. L., Andringa, K. K., Eccleston, H. B., and Bailey, S. M. (2008). Mitochondrial dysfunction and oxidative stress in the pathogenesis of alcohol- and obesity-induced fatty liver diseases. *Free Radic. Biol. Med.* 44 (7), 1259–1272. doi:10.1016/j.freeradbiomed.2007.12.029
- Mitchell, S., Vargas, J., and Hoffmann, A. (2016). Signaling via the NF κ B system. *Wiley Interdiscip. Rev. Syst. Biol. Med.* 8 (3), 227–241. doi:10.1002/wsbm.1331
- O-Uchi, J., Ryu, S. Y., Jhun, B. S., Hurst, S., and Sheu, S. S. (2014). Mitochondrial ion channels/transporters as sensors and regulators of cellular redox signaling. *Antioxid. Redox Signal* 21 (6), 987–1006. doi:10.1089/ars.2013.5681
- Pan, L. J., Zhang, Z. C., Zhang, Z. Y., Wang, W. J., Xu, Y., and Zhang, Z. M. (2012). Effects and mechanisms of store-operated calcium channel blockade on hepatic ischemia-reperfusion injury in rats. *World J. Gastroenterol.* 18 (4), 356–367. doi:10.3748/wjg.v18.i4.356
- Park, H. W., and Lee, J. H. (2014). Calcium channel blockers as potential therapeutics for obesity-associated autophagy defects and fatty liver pathologies. *Autophagy* 10 (12), 2385–2386. doi:10.4161/15548627.2014.984268
- Peng, W., Xu, Y., Han, D., Feng, F., Wang, Z., Gu, C., et al. (2020). Potential mechanism underlying the effect of matrine on COVID-19 patients revealed through network pharmacological approaches and molecular docking analysis. *Arch. Physiol. Biochem.* 129, 253–260. doi:10.1080/13813455.2020.1817944
- Periasamy, M., and Kalyanasundaram, A. (2007). SERCA pump isoforms: their role in calcium transport and disease. *Muscle Nerve* 35 (4), 430–442. doi:10.1002/mus.20745
- Peterson, T. R., Sengupta, S. S., Harris, T. E., Carmack, A. E., Kang, S. A., Balderas, E., et al. (2011). mTOR complex 1 regulates lipin 1 localization to control the SREBP pathway. *Cell* 146 (3), 408–420. doi:10.1016/j.cell.2011.06.034
- Prester, T., Talalay, P., Alam, J., Ahn, Y. I., Lee, P. J., and Choi, A. M. (1995). Parallel induction of heme oxygenase-1 and chemoprotective phase 2 enzymes by electrophiles and antioxidants: regulation by upstream antioxidant-responsive elements (ARE). *Mol. Med.* 1, 827–837. doi:10.1007/bf03401897
- Raghunath, A., Sundarraj, K., Nagarajan, R., Arfuso, F., Bian, J., Kumar, A. P., et al. (2018). Antioxidant response elements: Discovery, classes, regulation and potential applications. *Redox Biol.* 17, 297–314. doi:10.1016/j.redox.2018.05.002
- Rao, S. W., Duan, Y. Y., Zhao, D. S., Liu, C. J., Xu, S. H., Liang, D., et al. (2022). Integrative analysis of transcriptomic and metabolomic data for identification of pathways related to matrine-induced hepatotoxicity. *Chem. Res. Toxicol.* 35 (12), 2271–2284. doi:10.1021/acs.chemrestox.2c00264
- Rapizzi, E., Pinton, P., Szabadkai, G., Wieckowski, M. R., Vandecasteele, G., Baird, G., et al. (2002). Recombinant expression of the voltage-dependent anion channel enhances the transfer of Ca²⁺ microdomains to mitochondria. *J. Cell Biol.* 159 (4), 613–624. doi:10.1083/jcb.200205091
- Rieusset, J. (2017). Endoplasmic reticulum-mitochondria calcium signaling in hepatic metabolic diseases. *Biochim. Biophys. Acta Mol. Cell Res.* 1864 (6), 865–876. doi:10.1016/j.bbamer.2017.01.001
- Rinella, M. E., Elias, M. S., Smolak, R. R., Fu, T., Borensztajn, J., and Green, R. M. (2008). Mechanisms of hepatic steatosis in mice fed a lipogenic methionine choline-deficient diet. *J. Lipid Res.* 49 (5), 1068–1076. doi:10.1194/jlr.M800042-JLR200
- Saito, R., Suzuki, T., Hiramoto, K., Asami, S., Naganuma, E., Suda, H., et al. (2016). Characterizations of three major cysteine sensors of Keap1 in stress response. *Mol. Cell Biol.* 36 (2), 271–284. doi:10.1128/MCB.00868-15
- Sekiya, M., Hiraishi, A., Touyama, M., and Sakamoto, K. (2008). Oxidative stress induced lipid accumulation via SREBP1c activation in HepG2 cells. *Biochem. Biophys. Res. Commun.* 375 (4), 602–607. doi:10.1016/j.bbrc.2008.08.068
- Shi, D., Zhang, J., Qiu, L., Li, J., Hu, Z., and Zhang, J. (2013). Matrine inhibits infiltration of the inflammatory gr1(hi) monocyte subset in injured mouse liver through inhibition of monocyte chemoattractant protein-1. *Evid. Based Complement. Altern. Med.* 2013, 580673. doi:10.1155/2013/580673
- Shimano, H., and Sato, R. (2017). SREBP-regulated lipid metabolism: convergent physiology - divergent pathophysiology. *Nat. Rev. Endocrinol.* 13 (12), 710–730. doi:10.1038/nrendo.2017.91
- Shoshan-Barmatz, V., Krelin, Y., and Shteinfer-Kuzmine, A. (2018). VDAC1 functions in Ca²⁺ homeostasis and cell life and death in health and disease. *Cell Calcium* 69, 81–100. doi:10.1016/j.cecca.2017.06.007
- Snow, W. M., and Albenis, B. C. (2016). Neuronal gene targets of NF- κ B and their dysregulation in alzheimer's disease. *Front. Mol. Neurosci.* 9, 118. doi:10.3389/fnmol.2016.00118
- Song, B., Han, C., and Zhang, H. (2009). Toxicity of three *Sophora flavescens* ait alkaloids to mice. *Acta Bot. Boreali-Occidentalia Sin.* 29, 818–823.
- Stork, B. A., Dean, A., Ortiz, A. R., Saha, P., Putluri, N., Planas-Silva, M. D., et al. (2022). Calcium/calmodulin-dependent protein kinase 2 regulates hepatic fuel metabolism. *Mol. Metab.* 62, 101513. doi:10.1016/j.molmet.2022.101513
- Sun, X. Y., Jia, L. Y., Rong, Z., Zhou, X., Cao, L. Q., Li, A. H., et al. (2022). Research advances on matrine. *Front. Chem.* 10, 867318. doi:10.3389/fchem.2022.867318
- Szegezdi, E., Logue, S. E., Gorman, A. M., and Samali, A. (2006). Mediators of endoplasmic reticulum stress-induced apoptosis. *EMBO Rep.* 7 (9), 880–885. doi:10.1038/sj.embor.7400779
- Tang, B., Ai, Z., and Yao, S. (2013). Effects of Matrine on the expression of COX-2 and iNOS in rats with non-alcoholic fatty liver disease. *Chin. J. Clin. Electron. Ed.* 7, 2011–2015. doi:10.3877/cma.j.issn.1674-0785.2013.05.038
- Tang, B. D., Xia, X., Lv, X. F., Yu, B. X., Yuan, J. N., Mai, X. Y., et al. (2017). Inhibition of Orail-mediated Ca²⁺ entry enhances chemosensitivity of HepG2 hepatocarcinoma cells to 5-fluorouracil. *J. Cell Mol. Med.* 21 (5), 904–915. doi:10.1111/jcmm.13029
- Traaseth, N., Elfering, S., Solien, J., Haynes, V., and Giulivi, C. (2004). Role of calcium signaling in the activation of mitochondrial nitric oxide synthase and citric acid cycle. *Biochim. Biophys. Acta* 1658 (1–2), 64–71. doi:10.1016/j.bbabi.2004.04.015
- Vacca, A., Felli, M. P., Palermo, R., Di Mario, G., Calce, A., Di Giovine, M., et al. (2006). Notch3 and pre-TCR interaction unveils distinct NF- κ B pathways in T-cell development and leukemia. *Embo j.* 25 (5), 1000–1008. doi:10.1038/sj.emboj.7600996
- Wan, B., LaNoue, K. F., Cheung, J. Y., and Scaduto, R. C. (1989). Regulation of citric acid cycle by calcium. *J. Biol. Chem.* 264 (23), 13430–13439. doi:10.1016/s0021-9258(18)80015-1

- Wang, F., Yang, J. L., Yu, K. K., Xu, M., Xu, Y. Z., Chen, L., et al. (2015). Activation of the NF- κ B pathway as a mechanism of alcohol enhanced progression and metastasis of human hepatocellular carcinoma. *Mol. Cancer* 14 (1), 10. doi:10.1186/s12943-014-0274-0
- Wang, L., Lu, J., Sun, W., Gu, Y., Zhang, C., Jin, R., et al. (2017). Hepatotoxicity induced by radix Sophorae tonkinensis in mice and increased serum cholinesterase as a potential supplemental biomarker for liver injury. *Exp. Toxicol. Pathol.* 69 (4), 193–202. doi:10.1016/j.etp.2017.01.003
- Wang, Y., Zhang, S., Liu, J., Fang, B., Yao, J., and Cheng, B. (2018). Matrine inhibits the invasive and migratory properties of human hepatocellular carcinoma by regulating epithelial-mesenchymal transition. *Mol. Med. Rep.* 18 (1), 911–919. doi:10.3892/mmr.2018.9023
- Williams, G. S., Boyman, L., and Lederer, W. J. (2015). Mitochondrial calcium and the regulation of metabolism in the heart. *J. Mol. Cell Cardiol.* 78, 35–45. doi:10.1016/j.yjmcc.2014.10.019
- Wu, Y., Wang, Y., and Ma, X. (2014). Protective effects of matrine on acute ethanol-induced liver injury in mice. *Asia-Pacific Tradit. Med.* 10, 6–9.
- Xiao, F., Zhang, J., Zhang, C., and An, W. (2017). Hepatic stimulator substance inhibits calcium overflow through the mitochondria-associated membrane compartment during nonalcoholic steatohepatitis. *Lab. Invest.* 97 (3), 289–301. doi:10.1038/labinvest.2016.139
- Xiong, X., Wang, P., Duan, L., Liu, W., Chu, F., Li, S., et al. (2019). Efficacy and safety of Chinese herbal medicine Xiao Yao San in hypertension: a systematic review and meta-analysis. *Phytomedicine* 61, 152849. doi:10.1016/j.phymed.2019.152849
- Yang, Z., Yu, G. L., Zhu, X., Peng, T. H., and Lv, Y. C. (2022). Critical roles of FTO-mediated mRNA m6A demethylation in regulating adipogenesis and lipid metabolism: Implications in lipid metabolic disorders. *Genes Dis.* 9 (1), 51–61. doi:10.1016/j.gendis.2021.01.005
- Yang, Z., Gao, S., Yin, T., Kulkarni, K. H., Teng, Y., You, M., et al. (2010). Biopharmaceutical and pharmacokinetic characterization of matrine as determined by a sensitive and robust UPLC-MS/MS method. *J. Pharm. Biomed. Anal.* 51, 1120–1127. doi:10.1016/j.jpba.2009.11.020
- Yang, Z., Wang, L., and Wang, X. (2016). Matrine induces the hepatic differentiation of WB-F344 rat hepatic progenitor cells and inhibits Jagged 1/HES1 signaling. *Mol. Med. Rep.* 14 (4), 3841–3847. doi:10.3892/mmr.2016.5668
- Yang, Z. Y., Wang, L., Hou, Y. X., and Wang, X. B. (2013). Effects of matrine on oval cell-mediated liver regeneration and expression of RBP-jk and HES1. *Mol. Med. Rep.* 7 (5), 1533–1538. doi:10.3892/mmr.2013.1398
- Yin, H., Que, R., Liu, C., Ji, W., Sun, B., Lin, X., et al. (2018). Survivin-targeted drug screening platform identifies a matrine derivative WM-127 as a potential therapeutics against hepatocellular carcinoma. *Cancer Lett.* 425, 54–64. doi:10.1016/j.canlet.2018.03.044
- You, L., Yang, C., Du, Y., Liu, Y., Chen, G., Sai, N., et al. (2019). Matrine exerts hepatotoxic effects via the ROS-dependent mitochondrial apoptosis pathway and inhibition of nrf2-mediated antioxidant response. *Oxid. Med. Cell Longev.* 2019, 1045345. doi:10.1155/2019/1045345
- Younossi, Z. M., Wong, G., Anstee, Q. M., and Henry, L. (2023). The global burden of liver disease. *Clin. Gastroenterol. Hepatol.* 21 (8), 1978–1991. doi:10.1016/j.cgh.2023.04.015
- Yu, H. B., Zhang, H. F., Li, D. Y., Zhang, X., Xue, H. Z., and Zhao, S. H. (2011a). Matrine inhibits matrix metalloproteinase-9 expression and invasion of human hepatocellular carcinoma cells. *J. Asian Nat. Prod. Res.* 13 (3), 242–250. doi:10.1080/10286020.2010.551641
- Yu, H. C., Qin, H. Y., He, F., Wang, L., Fu, W., Liu, D., et al. (2011b). Canonical notch pathway protects hepatocytes from ischemia/reperfusion injury in mice by repressing reactive oxygen species production through JAK2/STAT3 signaling. *Hepatology* 54 (3), 979–988. doi:10.1002/hep.24469
- Yu, J. L., Li, J. H., Chengz, R. G., Ma, Y. M., Wang, X. J., and Liu, J. C. (2014). Effect of matrine on transforming growth factor β 1 and hepatocyte growth factor in rat liver fibrosis model. *Asian Pac J. Trop. Med.* 7 (5), 390–393. doi:10.1016/s1995-7645(14)60062-6
- Yuan, F., and Yang, Z. (2020). Influence of matrine on liver function and MAPK signaling pathway after hepatic ischemic reperfusion injury in rats. *J. Guangdong Pharm. Univ.* 36, 657–661. doi:10.16809/j.cnki.2096-3653.2020052003
- Yue, Z.-S., Ruan, B., Duan, J.-L., Han, H., and Wang, L. (2018). The role of the Notch signaling pathway in liver injury and repair. *J. Bio-X Res.* 1 (2), 95–104. doi:10.1097/jbr.0000000000000014
- Zeeshan, H. M., Lee, G. H., Kim, H. R., and Chae, H. J. (2016). Endoplasmic reticulum stress and associated ROS. *Int. J. Mol. Sci.* 17 (3), 327. doi:10.3390/ijms17030327
- Zhang, H. F., Shi, L. J., Song, G. Y., Cai, Z. G., Wang, C., and An, R. J. (2013). Protective effects of matrine against progression of hepatic stimulator substance diet-induced steatohepatitis by enhancing antioxidant and anti-inflammatory defences involving Nrf2 translocation. *Food Chem. Toxicol.* 55, 70–77. doi:10.1016/j.fct.2012.12.043
- Zhang, J., Li, Y., Jiang, S., Yu, H., and An, W. (2014). Enhanced endoplasmic reticulum SERCA activity by overexpression of hepatic stimulator substance gene prevents hepatic cells from ER stress-induced apoptosis. *Am. J. Physiol. Cell Physiol.* 306 (3), C279–C290. doi:10.1152/ajpcell.00117.2013
- Zhang, X. L., Xu, H. R., Chen, W. L., Chu, N. N., Li, X. N., Liu, G. Y., et al. (2009). Matrine determination and pharmacokinetics in human plasma using LC/MS/MS. *J. Chromatogr. B Anal. Technol. Biomed. Life Sci.* 877 (27), 3253–3256. doi:10.1016/j.jchromb.2009.08.026
- Zhao, Y. (2015). Effects of Matrine on infll ammatory factor in rats with liver injury of carbon tetrachloride. *Clin. J. Traditional Chin. Med.* 27, 727–728. doi:10.16448/j.cjtc.2015.0275
- Zheng, Y., Ding, Q., Wei, Y., Gou, X., Tian, J., Li, M., et al. (2021). Effect of traditional Chinese medicine on gut microbiota in adults with type 2 diabetes: a systematic review and meta-analysis. *Phytomedicine* 88, 153455. doi:10.1016/j.phymed.2020.153455
- Zhou, M., Li, Q., and Su, J. (2009). Effects of matrine on the expression of fas and fasL in liver tissue of mice injured by immune reaction. *China Trop. Med.* 9, 1445–1447.
- Zhou, Y., Wu, Y., Deng, L., Chen, L., Zhao, D., Lv, L., et al. (2014). The alkaloid matrine of the root of *Sophora flavescens* prevents arrhythmogenic effect of ouabain. *Phytomedicine* 21 (7), 931–935. doi:10.1016/j.phymed.2014.02.008
- Zhu, J., Zhu, J., Tang, F., Feng, Y., Zhou, Q., Jin, Q., et al. (2015). Influence of matrine on liver functions and TNF- α level following liver ischemic reperfusion injury in rats. *Chin. J. Clin. Res.* 28, 1147–1150. doi:10.13429/j.cnki.cjcr.2015.09.007

Glossary

Acc	Acetyl-coenzyme A-carboxylase	IRE1α	Inositol-requiring enzyme 1 α
ALT	Alanine aminotransferase	IMS	Intermembranous space
ARE	Antioxidant-responsive elements	IMM	Inner mitochondrial membrane
AST	Aspartate aminotransferase	IP3Rs	Inositol 1,4,5-trisphosphate receptors
ASIC-1	Acid-sensing ion channel 1	Keap1	kelch-like ECH-associated protein 1
ATF4	Transcription factor 4	L	Low
ATF6α	Activating transcription factor 6 α	M	Medium
Bax	Bcl-2-associated X protein	MCD	Methionine choline deficient
Bcl-2	B-cell lymphoma-2	MCU	Mitochondrial Ca ²⁺ uniporter
C	Control	MDA	Malondialdehyde
CAT	Catalase	MICU1/2	Mitochondrial Ca ²⁺ uptake 1/2
Ca²⁺	Calcium ion	MT	Matrine
CaMKII	Ca ²⁺ /Calmodulin-Dependent Protein Kinase II	mTORC1	mechanistic target of rapamycin complex 1
CHOP	C/EBP homologous protein	NASH	Nonalcoholic steatohepatitis
Cul3	Cullin3	NAFLD	Nonalcoholic fatty liver disease
COPII	Complexes in coat protein II	NAFLD	Non-alcoholic fatty liver disease
COX-2	Cyclooxygenase 2	NICD	Intracellular transmembrane domain
DHCR7	7-dehydrocholesterol reductase	Nrf2	Nuclear factor erythroid 2-related factor 2
DILI	Drug-induced liver injury	NSDHL	NAD-(P)-dependent steroid dehydrogenase-like
EASL	European Association for the Study of the Liver	NPS	Natural products
ECT	Electron transport chain	NF-κB	Nuclear factor kappa-B
ER	Endoplasmic reticulum	NQO-1	Quinone oxidoreductase-1
eIF2	eukaryotic initiation factor 2	OMM	Outer membrane of mitochondria
Fas	Fatty acid synthase	PKCδ	Protein kinase C delta
GRP75	Glucose-regulated protein 75	p-PERK	phosphor-plasmic reticulum kinase
GRP78	78 kDa glucose-regulated protein	Rbx1	Ring box protein 1
GST	Glutathione-S transferase	RyR	Ryanodine receptor
GPx	Glutathione peroxidase	ROS	Reactive oxygen species
H	High	RBP-J(κ)	Recombination signal binding protein (kappa) J
HES1	Hairy and enhancer of split 1	Scd1	Stearoyl-coenzyme A desaturase 1
HFD	High-fat die	SCAP	SREBP cleavage activating protein
HIRI	Hepatic ischemia-reperfusion injury	SD	Standard deviation
HMGCS1	3-hydroxy-3-methylglutaryl-coenzyme A synthase 1	SERCA	Sarco/endoplasmic reticulum Ca ²⁺ -ATPase
HO-1	Heme oxygenase-1	SOD	Superoxide dismutase
I	Intervention	SOC	Store-operated Ca ²⁺ channels
I²	I-squared	SRE	Sterol regulatory element
ICR mice	Institute of Cancer Research mice	SREBP	Sterol regulatory element binding protein
IL-1	Interleukin 1	sXBP1	spliced XBP1
IL-6	Interleukin 6	S1P	Site-1 proteases
		S2P	Site-2 proteases
		S1R	Sigma-1 receptor

TC	Total cholesterol
TCM	Traditional Chinese medicine
TG	Triglyceride
TGF-β	Transforming growth factor beta
TNF-α	Tumor necrosis factor alpha
UPR	Unfolded protein response
VDACs	Voltage-dependent anion channels
W	Week(s)
WHO	World Health Organization
XBPI	X-box-binding protein 1
95%CI	95% confidence interval